Atmos. Chem. Phys. Discuss., doi:10.5194/acp-2017-66, 2017
Manuscript under review for journal Atmos. Chem. Phys.
Discussion started: 6 March 2017
© Author(s) 2017. CC-BY 3.0 License.

Atmospheric Chemistry and Physics Discussions

A quantitative analysis of the reactions involved in stratospheric polar ozone depletion

Ingo Wohltmann[1], Ralph Lehmann[1], and Markus Rex[1]

[1]Alfred Wegener Institute for Polar and Marine Research, Potsdam, Germany

Correspondence to: I. Wohltmann (ingo.wohltmann@awi.de)

Abstract. We present a quantitative analysis of the chemical reactions involved in polar ozone depletion in the stratosphere, and of the relevant reaction pathways and cycles. While the reaction pathways and cycles involved in polar ozone depletion are well known, quantitative estimates of the importance of single reactions or reaction cycles are rare. In particular, there is no comprehensive and quantitative study of the reaction rates and cycles averaged over the polar vortex under conditions of heterogeneous chemistry so far. We show time series of reaction rates averaged over the polar vortex in winter and spring for all relevant reactions and indicate which reaction pathways and cycles are responsible for the vortex-averaged net change of the key species involved in ozone depletion, that is ozone, chlorine species (ClO_x, HCl, $ClONO_2$), bromine species, nitrogen species (HNO_3, NO_x) and hydrogen species (HO_x). For clarity, we focus on one Arctic winter (2004/2005) and one Antarctic winter (2006) in a layer in the lower stratosphere around 54 hPa. Mixing ratios and reaction rates are obtained from runs of the ATLAS Chemistry and Transport Model driven by ECMWF ERA Interim reanalysis data. An emphasis is put on the partitioning of the relevant chemical families (nitrogen, hydrogen, chlorine, bromine and odd oxygen) and activation and deactivation of chlorine.

1 Introduction

The chemistry of polar ozone depletion in the stratosphere has been the subject of ongoing research for the last 30 years (see e.g. review papers and text books by Wayne et al., 1995, Brasseur et al., 1999, Solomon, 1999, Brasseur and Solomon, 2005, Müller, 2011, and the reports of the World Meteorological Organization, WMO, 2011). In general, the chemistry of polar ozone depletion is understood very well (see e.g. the recent overview in Müller, 2011, or the special issue of the RECONCILE[1] project in this journal, von Hobe et al., 2013). Remaining issues, such as uncertainties in the formation pathways of Polar Stratospheric Clouds (PSCs) or uncertainties in the contribution of the different cloud types to chlorine activation (e.g. Lowe and MacKenzie, 2008; Peter and Grooß, 2012; Wohltmann et al., 2013), do not pose a serious challenge to the generally accepted basic theory.

While the reaction pathways and reaction cycles that are involved in ozone depletion are well known (e.g. Solomon, 1999; Müller, 2011), quantitative estimates of the importance of single reactions or reaction cycles are rare, and are limited to case studies or certain aspects of the chemical system (e.g. Grenfell et al., 2006) or apply mainly to conditions undisturbed by heterogeneous chemistry (e.g. Brasseur and Solomon, 2005).

[1]Reconciliation of essential process parameters for an enhanced predictability of Arctic stratospheric ozone loss and its climate interactions

Atmos. Chem. Phys. Discuss., doi:10.5194/acp-2017-66, 2017
Manuscript under review for journal Atmos. Chem. Phys.
Discussion started: 6 March 2017
© Author(s) 2017. CC-BY 3.0 License.

Atmospheric Chemistry and Physics Discussions

Here, we give a comprehensive overview of the temporal evolution of the vortex-averaged reaction rates and mixing ratios and associated reaction pathways and cycles for one Arctic winter (2004/2005) and one Antarctic winter (2006) in a layer in the lower stratosphere around 54 hPa. Vortex-averaged mixing ratios and reaction rates are obtained from runs of the ATLAS Chemistry and Transport Model (Wohltmann and Rex, 2009; Wohltmann et al., 2010). Since results cannot be based on direct observations due to a lack of measurements of the mixing ratios of minor species and reaction rates, only a model-based approach is feasible. The most important model parameters that influence the vortex-averaged rates are the initial mixing ratios, the laboratory measurements of the rate coefficients of the reactions (taken from Sander et al., 2011) and the meteorological data that drive the model, which are taken from the European Centre for Medium-Range Weather Forecasts (ECMWF) ERA Interim reanalysis (Dee et al., 2011). A detailed study of the uncertainties is outside the scope of this paper, but some of the major uncertainties will be noted. For a study of the uncertainties, see e.g. Kawa et al. (2009).

Good agreement of the modeled and observed mixing ratios for many species gives us confidence that our results represent the real atmosphere well in most cases (see Appendix). There was however a significant overestimation of HCl compared to measurements in our original model runs, which has also been observed in other models (Wegner et al., 2013). While we apply a correction based on changing the HCl solubility, which is a possible cause for this discrepancy, this introduces some uncertainty in our results (see Appendix).

While it is easy to identify the gross production or loss of a species by single reactions, it is difficult to identify what causes the net loss or production of a species (e.g. Lehmann, 2002). Often, the reactions that directly produce or remove a species of interest are part of a complicated chain of reactions, frequently involving reaction cycles. Many of these cycles will consume as much of a species as they produce (null cycles, equilibria), others will lead to a net loss of the species (loss cycles). Numerous loss cycles in the stratosphere are catalytic cycles, i.e. they destroy the species of interest with the help of another species that is constantly recycled in the loss cycle. To complicate things further, cycles may share species and reactions. Hence, it is of crucial importance to know the reaction cycles and pathways in the chemical system to actually understand the underlying reasons for the loss or production of a species, and these relationship are discussed in the following.

In Section 2, the methods and the model are introduced. The section contains a description of the ATLAS model and the setup of the runs and explains the method to obtain vortex-averaged reaction rates. In Section 3, we give an overview of the typical evolution of polar ozone chemistry in winter to provide a foundation for the following discussion. Section 4 discusses reactions and partitioning sorted by chemical families, that is nitrogen, hydrogen, chlorine, bromine and oxygen compounds. Section 5 contains the conclusions.

Results of this study are extensively used in a companion paper (Wohltmann et al., in preparation) to develop a fast model for polar ozone chemistry.

Atmos. Chem. Phys. Discuss., doi:10.5194/acp-2017-66, 2017
Manuscript under review for journal Atmos. Chem. Phys.
Discussion started: 6 March 2017
© Author(s) 2017. CC-BY 3.0 License.

Atmospheric Chemistry and Physics Discussions

2 Model and methods

2.1 Model overview

ATLAS is a global Chemistry and Transport Model (CTM) based on a Lagrangian (trajectory-based) approach. A detailed description of the model can be found in Wohltmann and Rex (2009) and Wohltmann et al. (2010). Updates to the chemistry module and polar stratospheric cloud module are described in Wohltmann et al. (2013). The model includes a gas-phase stratospheric chemistry module, heterogeneous chemistry on polar stratospheric clouds and a particle-based Lagrangian denitrification module. The chemistry module comprises 47 active species and more than 180 reactions. Absorption cross sections and rate coefficients are taken from recent JPL recommendations (Sander et al., 2011).

2.2 Model setup

Model runs are driven by meteorological data from the ECMWF ERA Interim reanalysis (Dee et al., 2011). The initial horizontal model resolution is 150 km. The runs use the hybrid pressure-potential temperature coordinate of the model, which is a pure potential temperature coordinate above 100 hPa. The vertical range of the model domain is 350 K to 1900 K. Vertical motion is driven by diabatic heating rates from ERA Interim. Two model runs are started, one for the northern hemispheric winter, and one for the southern hemispheric winter. The run for the northern hemisphere starts on 1 October 2004 and ends on 31 March 2005. The run for the southern hemisphere starts on 1 April 2006 and ends on 30 November 2006. Model data before 15 November 2004 or 1 May 2006 are not used for analysis to allow for a spin up of the mixing in the model and for a sufficiently stable vortex in the northern hemisphere.

In addition to the binary background aerosol, the model simulates three types of Polar Stratospheric Clouds, that is supercooled ternary $\mathrm{HNO_3/H_2SO_4/H_2O}$ solutions (STS), solid clouds composed of nitric acid trihydrate (NAT), and solid ice clouds.

The number density of NAT particles in the runs is set to 0.1 $\mathrm{cm^{-3}}$, the number density of ice particles is set to 0.01 $\mathrm{cm^{-3}}$ and the number density of the ternary solution droplets to 10 $\mathrm{cm^{-3}}$. A supersaturation of $\mathrm{HNO_3}$ over NAT of 10 (corresponding to about 3 K supercooling) is assumed to be necessary for the formation of the NAT particles. A detailed discussion of the rationale behind these choices can be found in Wohltmann et al. (2013). For ice particles, a supersaturation of 0.35 is assumed based on Microwave Limb Sounder (MLS) satellite measurements of $\mathrm{H_2O}$ (Waters et al., 2006) and ECMWF temperatures.

The treatment of conditions where both NAT and STS clouds are allowed to form has changed compared to Wohltmann et al. (2013). Since mixed NAT/STS clouds are commonly observed (e.g. Pitts et al., 2011), they can now form in the model to allow for a more realistic behaviour, see Nakajima et al. (2016) for details.

The settings for the polar stratospheric clouds largely favor the formation of liquid clouds (binary liquids and STS clouds) over the formation of NAT clouds and activation of chlorine predominantly occurs on liquid clouds in the model runs.

The Lagrangian particle model is used to simulate the nucleation, growth, sedimentation and evaporation of large NAT particles. These particles are formed with a nucleation rate of 7.8×10^{-6} particles per h and $\mathrm{cm^3}$ and an initial radius of 0.1 µm,

Atmos. Chem. Phys. Discuss., doi:10.5194/acp-2017-66, 2017
Manuscript under review for journal Atmos. Chem. Phys.
Discussion started: 6 March 2017
© Author(s) 2017. CC-BY 3.0 License.

Atmospheric Chemistry and Physics Discussions

wherever a supersaturation of 10 for HNO_3 is exceeded. Dehydration by falling ice particles is simulated by a simple new algorithm that irreversibly removes all ice above a given supersaturation, which is set to 0.7 here.

H_2O, N_2O, HCl, O_3, CO and HNO_3 are initialized from all measurements of the MLS instrument performed during 1 November 2004 and 1 May 2006, respectively. CH_4 is initialized from a monthly mean HALOE (Halogen Occultation Experiment) climatology (mean of the years 1991–2002) as a function of equivalent latitude and pressure (Grooß and Russell III, 2005). NO_x is initialized from the monthly mean HALOE data set by putting all NO_x into NO_2. $ClONO_2$ is calculated as the difference between Cl_y and HCl. Cl_y is taken from a Cl_y-N_2O tracer-tracer correlation from ER-2 aircraft and Triple balloon data (Grooß et al., 2002). As in Wohltmann et al. (2013), we increase the amount of $ClONO_2$ by 10 % at the expense of HCl, see the discussion there. $BrONO_2$ is assumed to contain all Br_y, which is taken from a Br_y-CH_4 relationship from ER-2 aircraft and Triple balloon data in Grooß et al. (2002). All values are scaled with a constant factor to give maximum values of 19.9 ppt.

2.3 Production and loss rates

Reaction rates are calculated for every reaction separately in the ATLAS model. For this purpose, one artificial species per reaction is introduced to the model, which is produced at the same rate as the other products of the reaction. For instance, a reaction of the type

$$\mathrm{A} + \mathrm{B} \rightarrow \mathrm{C} + \mathrm{D}$$

is modified to

$$\mathrm{A} + \mathrm{B} \rightarrow \mathrm{C} + \mathrm{D} + \mathrm{P}$$

where P is an artificial product species. The mixing ratio of the artificial product species is reset to zero every 24 hours. This way, P directly gives the 24 h averaged rates of production of the species C and D by this reaction and the 24 h averaged loss rates of the species A and B. The 24 h time period is used to capture the diurnal cycle of the photochemically active species. For technical reasons, heterogeneous reaction rates with the same chemical equation, but on different surface types are added together in a single reaction rate.

2.4 Vortex averages

Production and loss rates are averaged over all air parcels of the model inside the polar vortex, which are situated in a layer between 61.3 hPa and 47.4 hPa. The logarithmic mean level of this layer is at 54 hPa. The vortex edge is assumed to be situated at the 36 PVU contour of modified potential vorticity (PV) in the northern hemisphere and at the -36 PVU contour in the southern hemisphere. Modified PV is calculated from the potential vorticity field of the ERA Interim reanalysis according to Lait (1994), with $\theta_0 = 475$ K.

In order to obtain a more consistent picture of the ozone chemistry in the vortex, we exclude air parcels that experience a too high amount of mixing with extra-vortex air during the course of the model run. For that purpose, we initialize a “vortex

Atmos. Chem. Phys. Discuss., doi:10.5194/acp-2017-66, 2017
Manuscript under review for journal Atmos. Chem. Phys.
Discussion started: 6 March 2017
© Author(s) 2017. CC-BY 3.0 License.

Atmospheric Chemistry and Physics Discussions

tracer" as an artificial chemical species near the start of the model run (15 November in the northern hemisphere, 1 May in the southern hemisphere), which is set to 1 inside the vortex and to 0 outside the vortex. The vortex tracer is then transported and mixed like any other species in the model and can take any value between 0 and 1. We only include air parcels in the vortex mean, where the vortex tracer has a value greater than 0.7.

Without the vortex tracer, analysis would get much more complicated. An example may illustrate this: In the southern vortex, air masses rich in $\mathrm{NO_y}$ are mixed into the edge region of the vortex during the course of the winter, while in the core of the vortex, air masses are depleted of nitrogen species due to denitrification. This does not only lead to differences in mixing ratios of the nitrogen species over the vortex, but also to different reactions being important in different parts of the vortex. For example, while very low ozone values are reached in the core of the vortex since deactivation into $\mathrm{ClONO_2}$ is hindered, ozone values at the edge are higher and chlorine is also deactivated into $\mathrm{ClONO_2}$.

2.5 Different air masses

The $54\,\mathrm{hPa}$ level is not a material surface and we look at different air masses at different points of time, due to mixing, the movement of the isentropes relative to the pressure level and the additional sinking of the air masses relative to isentropes due to diabatic cooling. A similar caveat applies to the definition of the vortex edge. As a consequence of these transport effects, the temporal derivative of the vortex-averaged mixing ratio of a chemical species may deviate from the vortex-averaged chemical net production of this species.

Unfortunately, it is difficult to look at the same air mass over the course of several months, since an air mass with a well defined extent at the beginning of the winter will completely lose its identity due to mixing and transport during the course of the winter.

2.6 Equilibria

In many cases, two species X and Y with short lifetimes are in a fast equilibrium with each other, and will not change their mixing ratios if the external conditions do not change. For example, consider two fast reactions of the form

$$\mathrm{X} + \mathrm{Z}_1 \rightarrow \mathrm{Y} + \ldots$$

$$\mathrm{Y} + \mathrm{Z}_2 \rightarrow \mathrm{X} + \ldots$$

Then, assuming that the change of the mixing ratios is zero

$$\frac{\mathrm{d}[\mathrm{X}]}{\mathrm{d}t} = -k_1[\mathrm{X}][\mathrm{Z}_1] + k_2[\mathrm{Y}][\mathrm{Z}_2] = 0 \tag{1}$$

where $[\mathrm{X}]$ is the concentration of X and k_1 and k_2 are the reaction constants, we obtain equilibrium conditions like

$$\frac{[\mathrm{X}]}{[\mathrm{Y}]} = \frac{k_2[Z_2]}{k_1[Z_1]}. \tag{2}$$

Similar equations can be derived from more complex reaction systems. We use the equilibrium conditions in the following not only to show relationships between mixing ratios of different species, but also to determine the reactions involved in an

Atmos. Chem. Phys. Discuss., doi:10.5194/acp-2017-66, 2017
Manuscript under review for journal Atmos. Chem. Phys.
Discussion started: 6 March 2017
© Author(s) 2017. CC-BY 3.0 License.

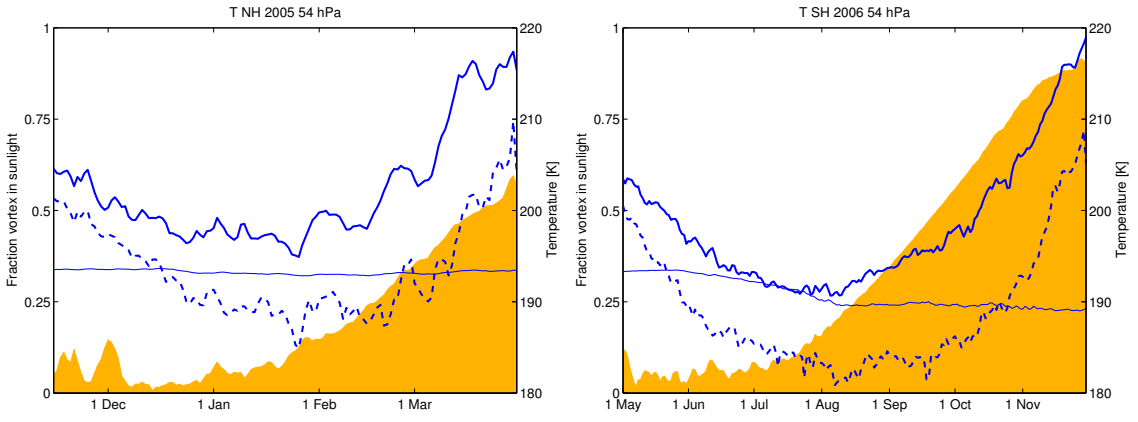

Figure 1. Vortex-averaged temperature (blue), vortex minimum temperature (dashed blue) and fraction of the vortex in sunlight (yellow) for the Arctic winter 2004/2005 (left) and the Antarctic winter 2006 (right) at 54 hPa. The thin blue line shows the threshold temperature for the formation of NAT clouds used in the model. The vortex tracer criterion described in the text was not applied (in contrast to all other figures).

equilibrium: For a given set of species, we start with a small set of reactions involved in the equilibrium derived from the vortex-averaged reaction rates, and calculate the mixing ratios of the species from the equilibrium conditions. Then, we compare these mixing ratios with the mixing ratios in the output of the model. If the mixing ratios determined by both methods do not agree with each other, we add reactions until we reach good agreement with a set of reactions as small as possible.

3 Short overview of the chemical evolution

The evolution of the chemistry of polar ozone depletion can be divided into several phases (see also Solomon, 1999, for an overview). For orientation, Figure 1 shows the evolution of temperature and sunlight in both hemispheres.

After the polar vortex forms in late autumn and early winter in response to the cooling of the atmosphere in the beginning of polar night, air masses in the vortex are well isolated from mid latitudes. In the first phase in early winter, chlorine, the main player in the chemistry of ozone depletion, is present mainly in the form of species that do not contribute to ozone depletion. These passive reservoir gases are mainly HCl and $ClONO_2$. Chemical activity is low due to the lack of sunlight in the polar night. This period lasts from the forming of the vortex until the first polar stratospheric clouds form.

In the second phase, HCl and $ClONO_2$ are transformed from passive reservoir gases to Cl_2 through heterogeneous reactions on the surface of polar stratospheric clouds (Solomon et al., 1986), which condense when temperatures in the polar night get cold enough. A second effect of the clouds can be the removal of large quantities of HNO_3 and H_2O by sedimentation (denitrification and dehydration), which can prolong ozone loss later in spring. In the model setup used here, activation predominantly occurs on liquid STS clouds and only to a lesser part on solid NAT clouds. Unfortunately, observations of PSCs are not detailed enough to sufficiently constrain the ratio of activation on STS versus NAT clouds, and there is also uncertainty in

Atmos. Chem. Phys. Discuss., doi:10.5194/acp-2017-66, 2017
Manuscript under review for journal Atmos. Chem. Phys.
Discussion started: 6 March 2017
© Author(s) 2017. CC-BY 3.0 License.

other parameters like size distribution, number densities and required supersaturation. However, chlorine activation and ozone loss are robust quantities with respect to changes in PSC parameterizations (Wohltmann et al., 2013).

The third phase starts when sunlight comes back, enabling catalytic cycles to destroy ozone in large quantities. Cl_2 is transformed to Cl and ClO by photolysis. Then ozone is removed mainly by the catalytic ClO dimer cycle and the catalytic ClO–BrO cycle. The second cycle makes ozone destruction sensitive to the amount of bromine and to bromine chemistry. At the same time, reactions that deactivate active chlorine and that are dependent on sunlight gain importance. Hence, there is a constant competition between activation and deactivation in this phase, as long as it is cold enough.

In the fourth phase, when temperatures rise in spring and PSCs dissolve, chlorine is deactivated into the reservoir gases again and ozone loss significantly decreases.

4 Budgets of the chemical families and chemical evolution arranged by families

4.1 Nitrogen species

NO_y is defined as the sum of all nitrogen containing species except for the long-lived source gas N_2O, which is the source of all other nitrogen species in the stratosphere. N_2O has both natural and anthropogenic sources in the troposphere (e.g. WMO, 2011; Montzka, 2012). The majority of NO_y is in the form of HNO_3 in the considered altitude range. This is due to the fact that removal of HNO_3 by photolysis and OH is not very efficient at these altitudes. The initial level of HNO_3 is about 13 to 14 ppb in both hemispheres and the initial NO_y is about 1 ppb higher. Figure 2 shows that the mixing ratio of HNO_3 (and NO_y) declines to about 3 ppb in February in the northern hemisphere and increases again in March due to transport. In contrast, HNO_3 decreases to about 0.5 ppb (with NO_y at 1 ppb) in the southern hemisphere after June. The rate of change of HNO_3 is not dominated by chemical changes, but by changes by denitrification, i.e. the irreversible removal of HNO_3 by sedimenting cloud particles, as shown in Figure 3. Denitrification is much more severe in the southern hemisphere due to the lower temperatures, leaving almost no NO_y (Figure 1). The amount of NO_y present in the other important nitrogen reservoir $ClONO_2$ is limited by the mixing ratio of Cl_y (less than 3.5 ppb). Thus, $ClONO_2$ never contributes more than about 25 % to NO_y.

NO_x is defined as the sum of the short-lived and reactive species NO, NO_2, NO_3 and $2\,N_2O_5$, which only form under sunlit conditions from the longer lived HNO_3. Only a small part of NO_y is in the form of NO_x under sunlit conditions, typically less than 2 ppb in the northern hemisphere and less than 0.75 ppb in the southern hemisphere. For the following discussion, it is reasonable to define an "extended" NO_x, which also includes $ClONO_2$ (and, much less importantly, $BrONO_2$ and HO_2NO_2), since these species are in very fast equilibria with the "classical" NO_x species under sunlit conditions.

The extended NO_x mixing ratios can be changed by a number of reactions. Vortex-averaged reaction rates of these reactions for the northern and southern hemisphere are shown in Figure 4. Extended NO_x is almost exclusively produced from HNO_3 under sunlit conditions by photolysis and reaction with OH

$$HNO_3 + h\nu \rightarrow NO_2 + OH \qquad \text{(R1)}$$

Atmos. Chem. Phys. Discuss., doi:10.5194/acp-2017-66, 2017
Manuscript under review for journal Atmos. Chem. Phys.
Discussion started: 6 March 2017
© Author(s) 2017. CC-BY 3.0 License.

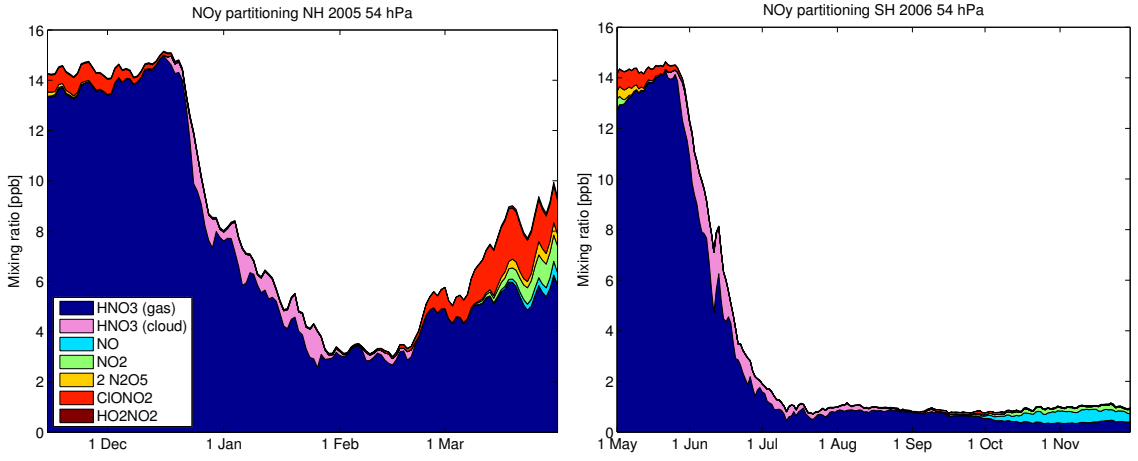

Figure 2. Vortex-averaged partitioning of NO_y species for the Arctic winter 2004/2005 (left) and the Antarctic winter 2006 (right) at 54 hPa. Species NO_3, $BrONO_2$, $ClNO_2$ and N are not shown due to their small mixing ratios.

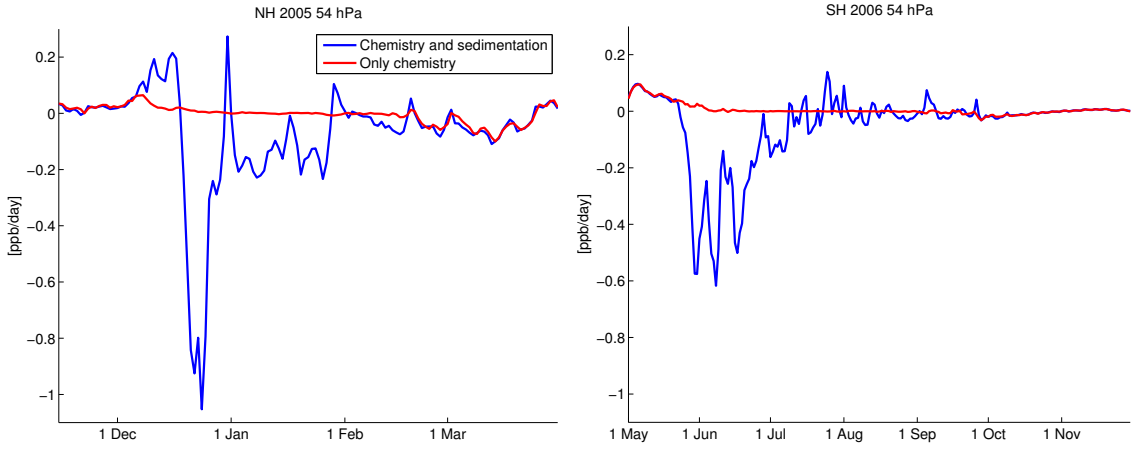

Figure 3. Vortex-averaged net chemical reaction rate of HNO_3 (red) for the Arctic winter 2004/2005 (left) and the Antarctic winter 2006 (right) at 54 hPa and sum of the vortex-averaged change by sedimentation and the net chemical reaction rate (blue).

Atmos. Chem. Phys. Discuss., doi:10.5194/acp-2017-66, 2017
Manuscript under review for journal Atmos. Chem. Phys.
Discussion started: 6 March 2017
© Author(s) 2017. CC-BY 3.0 License.

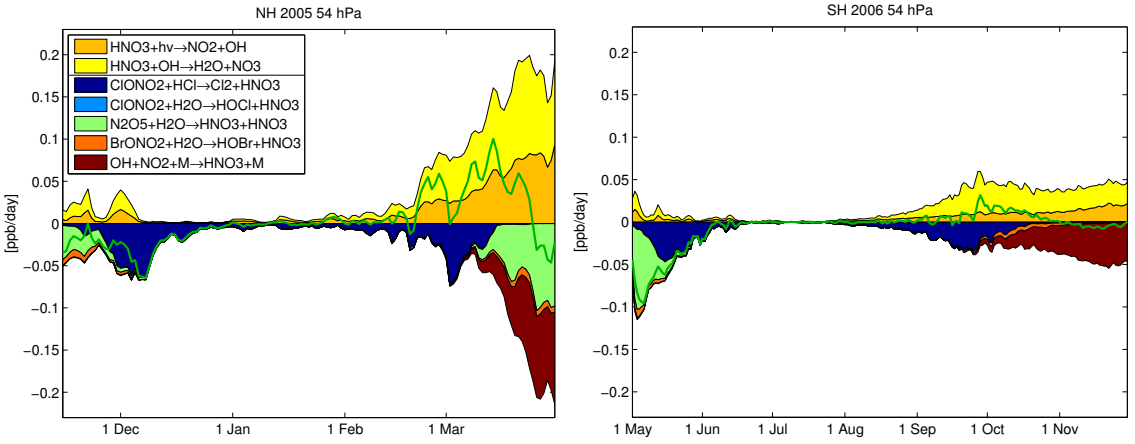

Figure 4. Vortex-averaged chemical reaction rates of reactions changing extended NO_x ($NO + NO_2 + NO_3 + 2\,N_2O_5 + ClONO_2 + BrONO_2 + HO_2NO_2$) for the Arctic winter 2004/2005 (left) and the Antarctic winter 2006 (right) at 54 hPa. Production reactions are shown positive and are separated by a line in the legend from the loss reactions, which are shown negative. The net change of extended NO_x is shown as a green line. Reactions with rates which cannot be distinguished from the zero line at plot resolution are not shown.

$$HNO_3 + OH \rightarrow H_2O + NO_3. \quad \text{(R2)}$$

The OH reaction contributes about 60 %–80 % to the production. Extended NO_x is lost to HNO_3 mainly by the heterogeneous reactions

$$N_2O_5 + H_2O \rightarrow HNO_3 + HNO_3 \quad \text{(R3)}$$

$$ClONO_2 + HCl \rightarrow Cl_2 + HNO_3 \quad \text{(R4)}$$

and by the gas-phase reaction

$$OH + NO_2 + M \rightarrow HNO_3 + M. \quad \text{(R5)}$$

The reaction $N_2O_5 + H_2O$ proceeds on the background aerosol, not only when polar stratospheric clouds are present. When sunlight comes back to the vortex in spring, reactions R1–R2 are not in equilibrium with R3–R5 and produce extended NO_x from HNO_3. Due to the denitrified conditions in the southern hemisphere, much less NO_x is produced there.

Note that the introduction of an extended NO_x does not work very well under polar night conditions, since $ClONO_2$ is not in equilibrium with the classical NO_x then, which can be seen in the fact that extended NO_x is lost in polar night due to heterogeneous reaction of $ClONO_2$, although no NO or NO_2 is present.

Atmos. Chem. Phys. Discuss., doi:10.5194/acp-2017-66, 2017
Manuscript under review for journal Atmos. Chem. Phys.
Discussion started: 6 March 2017
© Author(s) 2017. CC-BY 3.0 License.

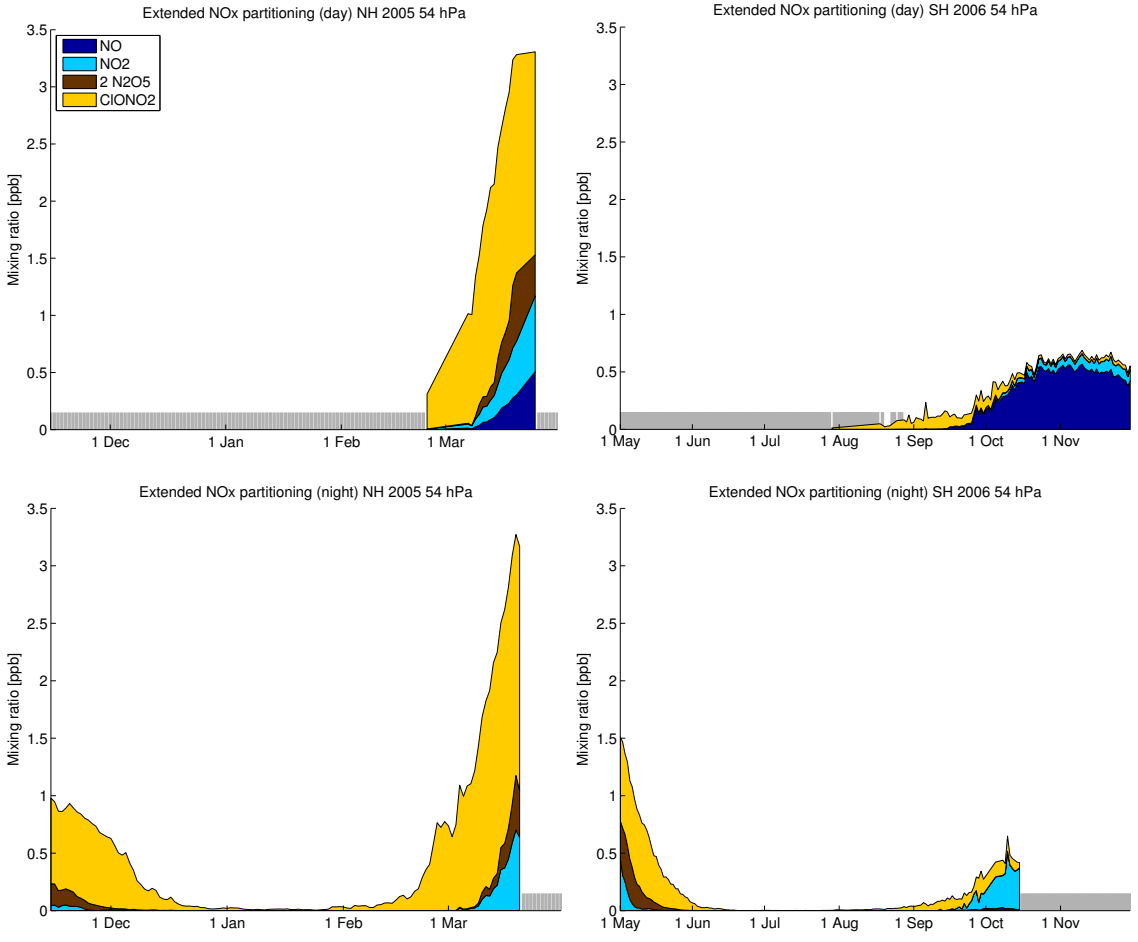

Figure 5. Vortex-averaged partitioning of extended NO_x species for the Arctic winter 2004/2005 (left) and the Antarctic winter 2006 (right) at 54 hPa. Top row: Daytime averages (parts of the vortex where the solar zenith angle is smaller than 80°). Bottom row: Nighttime averages (parts of the vortex where the solar zenith angle is larger than 100°). Days without sufficient data for averaging are not shown (grey bars).

Atmos. Chem. Phys. Discuss., doi:10.5194/acp-2017-66, 2017
Manuscript under review for journal Atmos. Chem. Phys.
Discussion started: 6 March 2017
© Author(s) 2017. CC-BY 3.0 License.

Atmospheric Chemistry and Physics Discussions

Figure 5 shows the partitioning of extended NO_x during daytime and at night. Daytime averages are defined over the parts of the vortex where the solar zenith angle is smaller than 80° and nighttime averages are defined over parts of the vortex where the solar zenith angle is larger than 100°. Except for early winter, NO_x proper is only present in appreciable quantities after the start of March or October, respectively. During daytime, the partitioning between NO and NO_2 is so fast that steady state conditions can be assumed. The three reactions that determine the equilibrium are

$$O_3 + NO \rightarrow NO_2 + O_2 \quad \text{(R6)}$$

$$ClO + NO \rightarrow Cl + NO_2 \quad \text{(R7)}$$

$$NO_2 + h\nu \rightarrow NO + O. \quad \text{(R8)}$$

Figure 6 shows the formation and loss rates of NO to illustrate this (the corresponding plots for NO_2 look identical, but mirrored). The equilibrium condition derived from these reactions is

$$\frac{[NO]}{[NO_2]} = \frac{k_{R8}}{k_{R6}[O_3] + k_{R7}[ClO]}. \quad (3)$$

In the southern hemisphere during daytime, the fraction of NO compared to NO_2 is much higher than in the northern hemisphere (80 %–90 % NO and 10 %–20% NO_2 in the southern hemisphere, and 20 %–40 % NO and 60 %–80 % NO_2 in the northern hemisphere). The higher NO levels are caused by the much lower ozone levels in the southern hemisphere (see Figure 19), which shifts the equilibrium by hindering the $O_3 + NO$ reaction. At night, no NO is present, since the reaction $NO_2 + h\nu$ does not take place. NO_3 only plays a negligible role for the budget of NO_x due to the fast reaction into NO_2 by

$$NO_3 + h\nu \rightarrow NO_2 + O \quad \text{(R9)}$$

during daytime and into N_2O_5 at night (see discussion of R13).

Despite the relatively low mixing ratios, NO_x plays an important role in ozone chemistry. In addition to the equilibrium between NO and NO_2, there is a fast equilibrium between NO_2 and $ClONO_2$ under sunlit conditions, so that all three species are coupled. $ClONO_2$ is to a good approximation in an equilibrium between

$$ClONO_2 + h\nu \rightarrow Cl + NO_3 \quad \text{(R10)}$$

$$\rightarrow ClO + NO_2 \quad \text{(R11)}$$

and

$$ClO + NO_2 + M \rightarrow ClONO_2 + M. \quad \text{(R12)}$$

Atmos. Chem. Phys. Discuss., doi:10.5194/acp-2017-66, 2017
Manuscript under review for journal Atmos. Chem. Phys.
Discussion started: 6 March 2017
© Author(s) 2017. CC-BY 3.0 License.

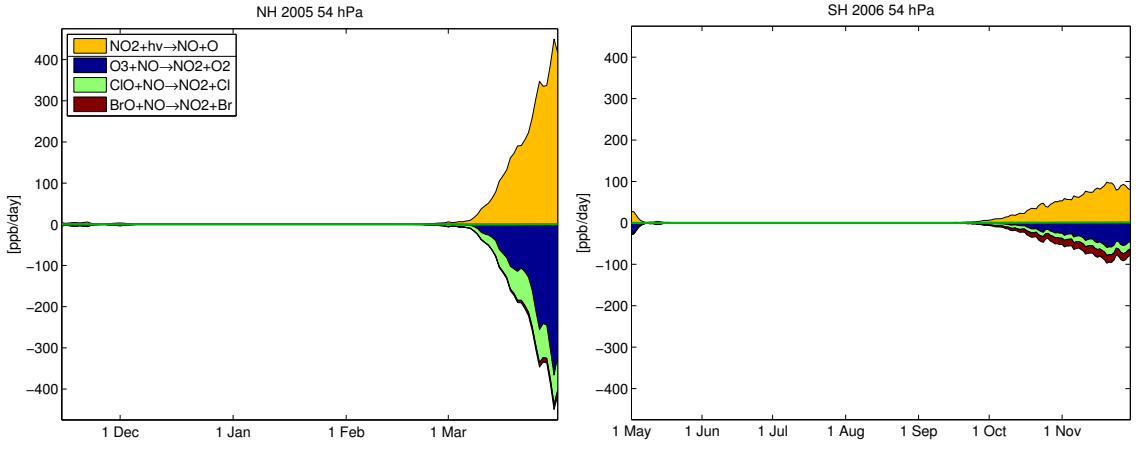

Figure 6. Vortex-averaged chemical reaction rates of reactions changing NO for the Arctic winter 2004/2005 (left) and the Antarctic winter 2006 (right) at 54 hPa to illustrate NO_x partitioning. Production reactions are shown positive and are separated by a line in the legend from the loss reactions, which are shown negative. The net change of NO is shown as a green line.

Reaction R10 is the dominating branch of the $ClONO_2$ photolysis. The equilibrium condition for $ClONO_2$ can be written as

$$[ClO][NO_2] = \frac{k_{R10} + k_{R11}}{k_{R12}}[ClONO_2]. \quad (4)$$

Alternatively, since NO and NO_2 are in equilibrium, this can also be expressed in terms of NO

$$[ClO][NO] = \frac{(k_{R10} + k_{R11})k_{R8}[ClONO_2]}{k_{R12}(k_{R6}[O_3] + k_{R7}[ClO])}. \quad (5)$$

Production of NO_x from HNO_3 in spring will increase NO_2. In turn, $ClONO_2$ will increase almost instantly at the expense of NO_2 to match the equilibrium condition again. In this sense, $ClONO_2$ is produced from HNO_3 via NO_x in spring. This is an important deactivation pathway for active chlorine in the northern hemisphere, since it consumes ClO.

There is a striking difference in $ClONO_2$ production in spring between the northern and southern hemisphere. While $ClONO_2$ increases to 2 ppb in the northern hemisphere, it stays below 0.1 ppb in the southern hemisphere due to the strongly denitrified conditions there. The hindrance of the deactivation path via $ClONO_2$ under denitrified conditions prolongs the period of ozone loss, since the other deactivation path via the reaction $Cl + CH_4$ is only effective under low ozone levels (see section 4.3.2). $ClONO_2$ stays relatively constant in March in the northern hemisphere after the initial increase, since the decrease in ClO is compensated by an increase in NO_2. In the southern hemisphere, ClO drops to even lower values after October due to missing ozone.

The mixing ratio of N_2O_5 is governed by

$$NO_2 + NO_3 + M \rightarrow N_2O_5 + M \quad (R13)$$

Atmos. Chem. Phys. Discuss., doi:10.5194/acp-2017-66, 2017
Manuscript under review for journal Atmos. Chem. Phys.
Discussion started: 6 March 2017
© Author(s) 2017. CC-BY 3.0 License.

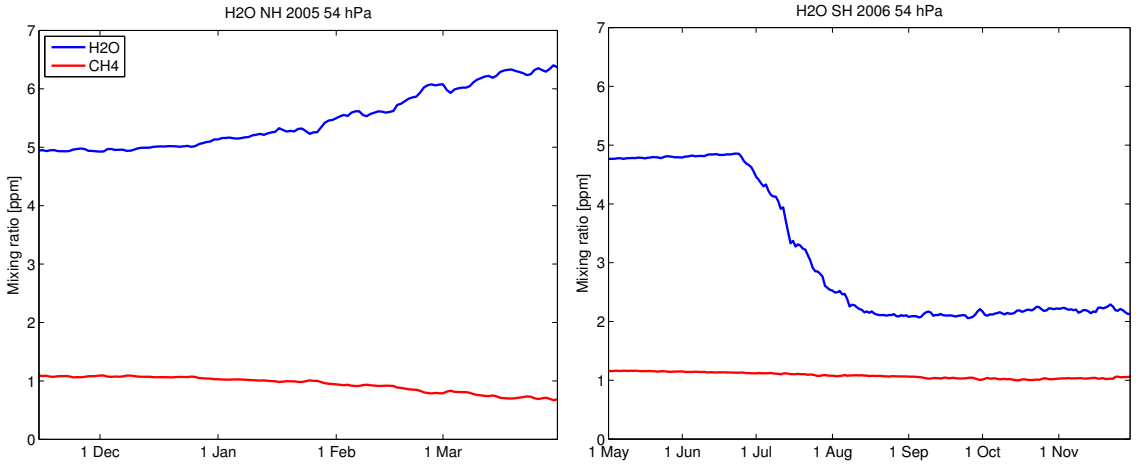

Figure 7. Vortex-averaged mixing ratios of H_2O and CH_4 for the Arctic winter 2004/2005 and the Antarctic winter 2006 at 54 hPa.

$$N_2O_5 + h\nu \rightarrow NO_2 + NO_3 \quad \text{(R14)}$$

$$N_2O_5 + H_2O \rightarrow HNO_3 + HNO_3. \quad \text{(R3)}$$

At night N_2O_5 is produced slowly by reaction R13, with NO_3 produced by

$$NO_2 + O_3 \rightarrow NO_3 + O_2. \quad \text{(R15)}$$

During daytime, no N_2O_5 is produced, since the NO_3 produced by reactions R10 and R15 is easily photolyzed. However, N_2O_5 is only slowly depleted during daytime, so that N_2O_5 levels during daytime and at night are comparable in the northern hemisphere (up to 30 % of classical NO_x is in N_2O_5). In the southern hemisphere, low ozone levels hinder the production of N_2O_5. The produced N_2O_5 can react back to the reservoir HNO_3 via reaction R3 (see Figure 4).

4.2 Hydrogen species

The sources for $HO_x = OH + HO_2$ are mainly H_2O, CH_4 and HNO_3. The source for stratospheric water is humid tropospheric air "freeze-dried" at the tropopause and sources for CH_4 are both natural (wetlands) and anthropogenic (e.g. WMO, 2011; Montzka, 2012). CH_4 is slowly oxidized to H_2O in the stratosphere (see also below). Figure 7 shows that the mixing ratio for H_2O is between 2 ppm and 6 ppm and that CH_4 has a mixing ratio of about 1 ppm. The decrease of H_2O in July in the southern hemisphere is caused by dehydration by sedimenting cloud particles, similar to the situation for HNO_3. The northern hemisphere is not cold enough for the formation of a significant amount of ice clouds.

Production and loss processes of HO_x are fairly complicated (Hanisco, 2003). Figure 8 shows the production and loss rates of an extended HO_x, where we have included some species that are not a net source or sink of HO_x over a diurnal cycle

Atmos. Chem. Phys. Discuss., doi:10.5194/acp-2017-66, 2017
Manuscript under review for journal Atmos. Chem. Phys.
Discussion started: 6 March 2017
© Author(s) 2017. CC-BY 3.0 License.

Atmospheric Chemistry and Physics Discussions

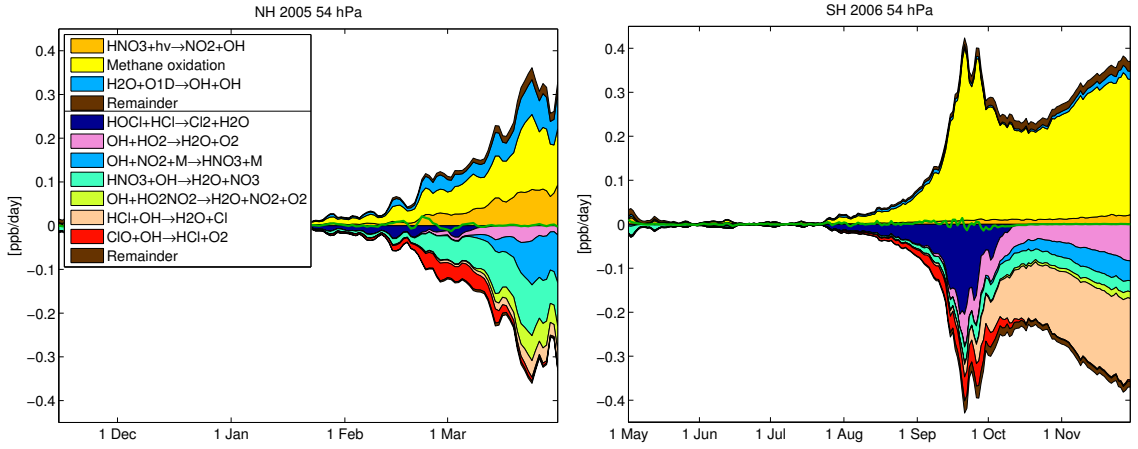

Figure 8. Vortex-averaged chemical reaction rates of reactions changing extended HO_x ($OH + HO_2 + H + HOCl + HOBr + HO_2NO_2$) for the Arctic winter 2004/2005 (left) and the Antarctic winter 2006 (right) at 54 hPa. Production reactions are shown positive and are separated by a line in the legend from the loss reactions, which are shown negative. The net change of extended HO_x is shown as a green line. Methane oxidation is modelled by simplified net reactions in ATLAS, the reactions denoted as methane oxidation in the legend are $Cl + CH_4 \rightarrow HCl + CH_2O + HO_2$ and $Cl + CH_2O \rightarrow HCl + CO + HO_2$.

(extended HO_x = $OH + HO_2 + H + HOCl + HOBr + HO_2NO_2$). Particularly in the southern hemisphere, production from CH_4 oxidation, which can be initiated by

$$X + CH_4 \rightarrow XH + CH_3 \quad \text{(R16)}$$

with $X = Cl$, $O(^1D)$, OH and then continues with a complicated chain of reactions involving CH_2O (see Hanisco, 2003, for more details), plays an important role. The maximum yield of this reaction chain is 4 HO_x per CH_4, but the yield is normally lower (Hanisco, 2003). For example, the HCl formed by R16 with $X = Cl$ lowers the yield of the reaction chain starting with this reaction because of the reaction

$$HCl + OH \rightarrow H_2O + Cl. \quad \text{(R17)}$$

Reaction of water with $O(^1D)$

$$H_2O + O(^1D) \rightarrow OH + OH \quad \text{(R18)}$$

and photolysis of HNO_3

$$HNO_3 + h\nu \rightarrow NO_2 + OH \quad \text{(R1)}$$

can also produce HO_x. Sinks are the recombination into water

$$OH + HO_2 \rightarrow H_2O + O_2 \quad \text{(R19)}$$

Atmos. Chem. Phys. Discuss., doi:10.5194/acp-2017-66, 2017
Manuscript under review for journal Atmos. Chem. Phys.
Discussion started: 6 March 2017
© Author(s) 2017. CC-BY 3.0 License.

Atmospheric Chemistry and Physics Discussions

and the reactions

$$OH + NO_2 + M \rightarrow HNO_3 + M \quad (R5)$$

$$HNO_3 + OH \rightarrow H_2O + NO_3 \quad (R2)$$

$$ClO + OH \rightarrow HCl + O_2. \quad (R20)$$

HO_x is in equilibrium with $HOCl$ under sunlit conditions and when chlorine is activated

$$HOCl + h\nu \rightarrow Cl + OH \quad (R21)$$

$$ClO + HO_2 \rightarrow HOCl + O_2. \quad (R22)$$

Hence, the heterogeneous reaction

$$HOCl + HCl \rightarrow Cl_2 + H_2O \quad (R23)$$

is also a sink for HO_x.

HO_x levels are about 1 to 4 ppt under sunlit conditions in both hemispheres (Figure 9). At night, no HO_x is present, since there is no production and HO_x recombines into water and HNO_3 (Figure 8). $HOCl$ can reach mixing ratios of up to 0.15 ppb in both hemispheres, as long as chlorine is activated. Figure 9 shows that HO_x does not simply scale with the amount of sunlight, HNO_3, H_2O and CH_4: In the southern hemisphere, HO_x shows a peak under conditions of both chlorine activation and sunlight, related to the fact that reactions like $Cl + CH_4$ and $HOCl + HCl$ play a role in HO_x production.

Figure 9 also shows the partitioning of HO_x. Similar to NO_x, there is a fast equilibrium between OH and HO_2. The partitioning inside HO_x is determined mainly by

$$HOCl + h\nu \rightarrow Cl + OH \quad (R21)$$

$$ClO + HO_2 \rightarrow HOCl + O_2 \quad (R22)$$

$$ClO + OH \rightarrow Cl + HO_2 \quad (R24)$$

$$O_3 + HO_2 \rightarrow OH + 2\,O_2 \quad (R25)$$

Atmos. Chem. Phys. Discuss., doi:10.5194/acp-2017-66, 2017
Manuscript under review for journal Atmos. Chem. Phys.
Discussion started: 6 March 2017
© Author(s) 2017. CC-BY 3.0 License.

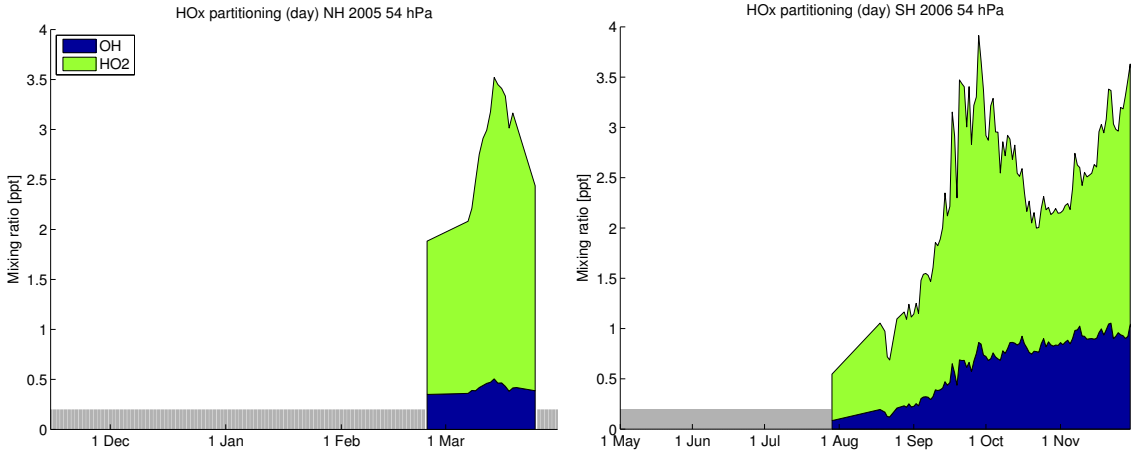

Figure 9. Vortex-averaged partitioning of HO_x species for the Arctic winter 2004/2005 (left) and the Antarctic winter 2006 (right) at 54 hPa. Daytime averages (parts of the vortex where the solar zenith angle is smaller than 80°). Nighttime averages are near zero and not shown. Days without sufficient data for averaging are not shown (grey bars).

$$O_3 + OH \rightarrow HO_2 + O_2 \tag{R26}$$

$$NO + HO_2 \rightarrow NO_2 + OH. \tag{R27}$$

Figure 10 shows the rates of HO_2 production and loss to illustrate that (the corresponding plots for OH look similar, but mirrored, and $ClO + HO_2$ is replaced by $HOCl + h\nu$). The production and loss rates of HO_x proper are dominated by the reactions R21 and R22 which form the equilibrium with HOCl (not shown).

The equilibrium is mainly on the side of HO_2 in both hemispheres. The fraction of OH is somewhat higher in the southern hemisphere (about 20 %–40 %) than in the northern hemisphere (about 10 %–20 %). Absolute OH levels are of relatively similar magnitude (up to 1 ppt in the southern hemisphere and up to 0.5 ppt in the northern hemisphere).

Equations for the equilibrium values of OH, HO_2 and HOCl can be derived from reactions R21 to R27. The ratio of OH and HO_2 under sunlit conditions in the northern hemisphere and in the southern hemisphere before mid-September is in good approximation given by

$$\frac{[OH]}{[HO_2]} = \frac{k_{R25}[O_3] + k_{R22}[ClO] + k_{R27}[NO]}{k_{R26}[O_3] + k_{R24}[ClO]}. \tag{6}$$

That is, the ratio depends only on O_3, ClO and NO. The equation can be simplified to

$$\frac{[OH]}{[HO_2]} = \frac{k_{R25}[O_3] + k_{R22}[ClO]}{k_{R26}[O_3] + k_{R24}[ClO]} \tag{7}$$

Atmos. Chem. Phys. Discuss., doi:10.5194/acp-2017-66, 2017
Manuscript under review for journal Atmos. Chem. Phys.
Discussion started: 6 March 2017
© Author(s) 2017. CC-BY 3.0 License.

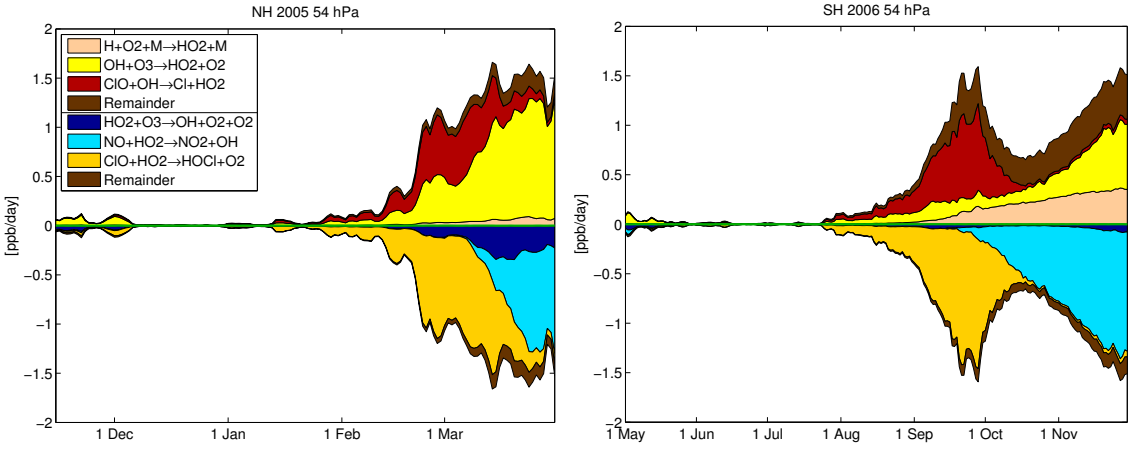

Figure 10. Vortex-averaged chemical reaction rates of reactions changing HO_2 for the Arctic winter 2004/2005 (left) and the Antarctic winter 2006 (right) at 54 hPa to illustrate HO_x partitioning. Production reactions are shown positive and are separated by a line in the legend from the loss reactions, which are shown negative. The net change of HO_2 is shown as a green line.

under conditions when chlorine is activated and no NO is present (before March and mid-September, respectively) and to

$$\frac{[OH]}{[HO_2]} = \frac{k_{R25}[O_3] + k_{R27}[NO]}{k_{R26}[O_3]} \tag{8}$$

in spring (end of March) in the northern hemisphere. In the southern hemisphere, the change between conditions rich in ClO_x and rich in NO_x can be seen in a change in the relative partitoning (Figure 9). A similar discussion and expressions for mid-latitudes can be found in Cohen et al. (1994).

Under sunlit conditions and when chlorine is activated, the equilibrium of HOCl is given by

$$[HOCl] = \frac{k_{R22}}{k_{R21}}[ClO][HO_2]. \tag{9}$$

At night, HOCl remains constant (except for heterogeneous processing), since neither the photolysis reaction nor the $ClO + HO_2$ reaction can proceed.

HO_x is relevant for ozone depletion, since the reactions $HCl + OH \rightarrow H_2O + Cl$ and $ClO + OH \rightarrow HCl + O_2$ play a role in chlorine activation and deactivation (note that the second reaction differs from reaction R24 in the products). In addition, chlorine can be activated by the heterogeneous $HOCl + HCl$ reaction.

4.3 Chlorine species

4.3.1 Overview and partitioning

When the polar vortex forms, the majority of chlorine is present in the form of HCl and the remainder is present in the other important reservoir gas $ClONO_2$. Figure 11 shows the partitioning between the various inorganic chlorine species (Cl_y). The

Atmos. Chem. Phys. Discuss., doi:10.5194/acp-2017-66, 2017
Manuscript under review for journal Atmos. Chem. Phys.
Discussion started: 6 March 2017
© Author(s) 2017. CC-BY 3.0 License.

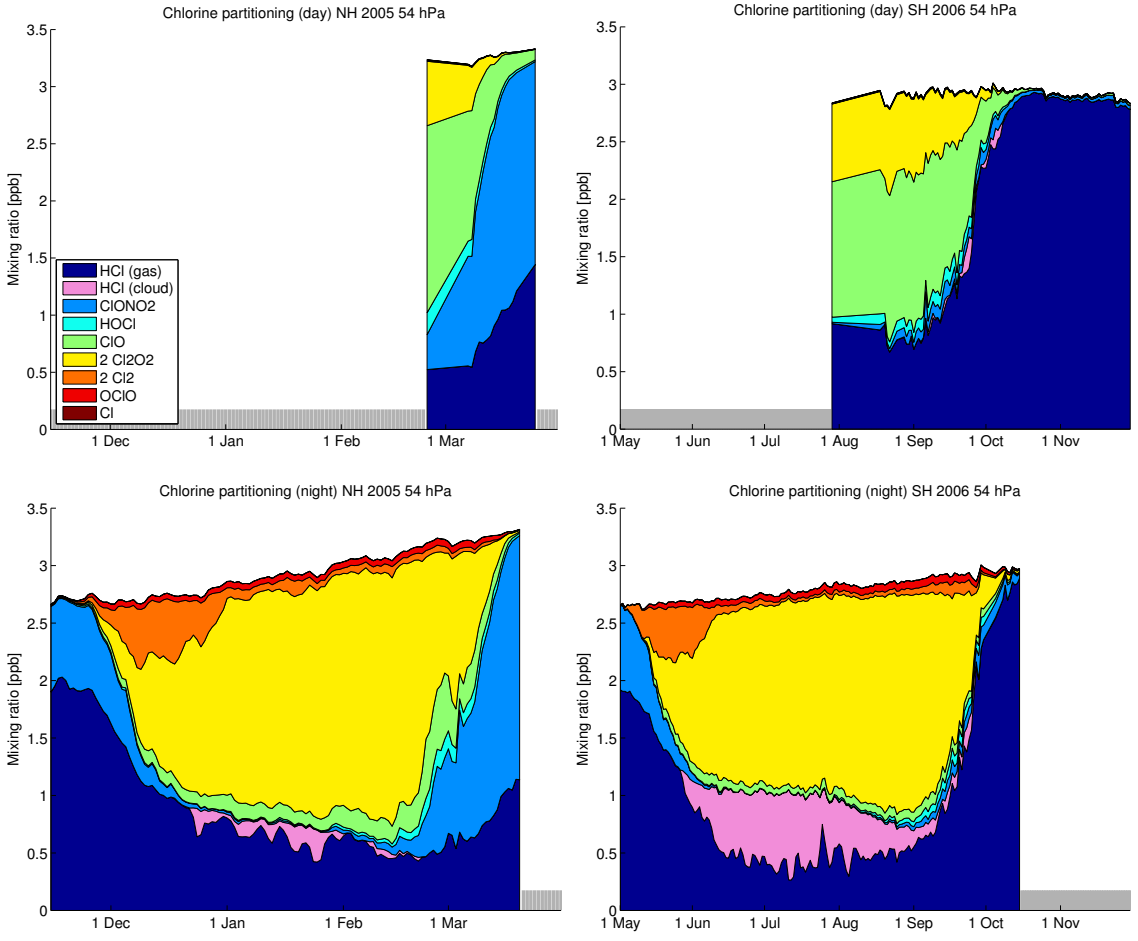

Figure 11. Vortex-averaged partitioning of inorganic chlorine species (Cl_y) for the Arctic winter 2004/2005 (left) and the Antarctic winter 2006 (right) at 54 hPa. Top row: Daytime averages (parts of the vortex where the solar zenith angle is smaller than 80°). Bottom row: Nighttime averages (parts of the vortex where the solar zenith angle is larger than 100°). Days without sufficient data for averaging are not shown (grey bars). Species $ClNO_2$ and BrCl are not shown due to their small mixing ratios.

available amount of Cl_y is about 2.7 to 3.3 ppb in the considered altitude range (the increase is due to transport from above). In both hemispheres, the initial mixing ratio of HCl is about 2 ppb (75 % of Cl_y) and the initial mixing ratio of $ClONO_2$ is about 0.7 ppb. Cl_y is produced by photolysis and reaction with $O(^1D)$ from chlorofluorocarbons (CFCs), hydrochlorofluorocarbons (HCFCs) and similar species of mainly anthropogenic origin (e.g. WMO, 2011; Montzka, 2012).

In early winter, passive reservoir gases HCl and $ClONO_2$ are transformed to Cl_2 through heterogeneous reactions on the surface of polar stratospheric clouds (starting in December in the northern hemisphere and May in the southern hemisphere). Since the major reaction that transforms the reservoir gases to Cl_2 is $HCl + ClONO_2$ (e.g. Solomon et al., 1986, see also section 4.3.2), the amount of chlorine that can be activated is limited by the mixing ratio of the less abundant $ClONO_2$. While

Atmos. Chem. Phys. Discuss., doi:10.5194/acp-2017-66, 2017
Manuscript under review for journal Atmos. Chem. Phys.
Discussion started: 6 March 2017
© Author(s) 2017. CC-BY 3.0 License.

some $ClONO_2$ can be regenerated by the reaction $ClO+NO_2+M$ and some HCl can be activated by the reaction $HOCl+HCl$, this is not sufficient to remove all HCl over the course of the winter, and total HCl mixing ratios consistently stay larger than 0.5 ppb in our model runs, while $ClONO_2$ decreases to near zero values. Due to the applied correction to the HCl solubility (see Appendix), up to 0.5 ppb of HCl are dissolved in STS droplets in the southern hemisphere.

When sunlight starts to come back, Cl_2 is quickly transformed to the active chlorine species ClO and its dimer Cl_2O_2 by photolysis of Cl_2

$$Cl_2 + h\nu \rightarrow Cl + Cl \tag{R28}$$

immediately followed by the reaction

$$Cl + O_3 \rightarrow ClO + O_2 \tag{R29}$$

to produce ClO. The time between first activation and the first sunlight becomes apparent in a Cl_2 peak in December and May in Figure 11.

Under polar conditions, the dimer of ClO plays an important role. Reactions that determine the ratio of ClO and its dimer Cl_2O_2 are

$$ClO + ClO + M \rightarrow Cl_2O_2 + M \tag{R30}$$

$$Cl_2O_2 + h\nu + M \rightarrow 2\,Cl + O_2 + M \tag{R31}$$

$$Cl_2O_2 + M \rightarrow ClO + ClO + M. \tag{R32}$$

Reactions R30 and R31 are also part of the ClO dimer ozone loss cycle (see section 4.5). Note that reaction R31 includes an intermediate step over ClOO not shown here. Figure 12 shows the partitioning of $ClO_x = ClO + 2\,Cl_2O_2$. Active chlorine is mainly present in the form of Cl_2O_2 at night and in the form of ClO during daytime. At night, only small levels of ClO are maintained by the interplay between the forward and backward reaction R32 and R30 (see also Wayne et al., 1995, p. 2836). During daytime, most Cl_2O_2 is photolyzed into Cl which reacts to ClO and there is an equilibrium between ClO and Cl_2O_2. About 70 % of ClO_x is present as ClO during daytime.

When chlorine is activated from December to the beginning of March in the northern hemisphere and from May to September in the southern hemisphere, ozone is removed by the ClO dimer cycle and the ClO–BrO cycle (see section 4.5). ClO_x peaks at about 2.4 ppb in the northern hemisphere and at about 2.0 ppb in the southern hemisphere.

4.3.2 Reservoir HCl

Figure 13 shows the time evolution of the vortex-averaged reaction rates of all relevant reactions that change HCl. In early winter (up to the end of December in the northern hemisphere and up to the end of July in the southern hemisphere), HCl is

Atmos. Chem. Phys. Discuss., doi:10.5194/acp-2017-66, 2017
Manuscript under review for journal Atmos. Chem. Phys.
Discussion started: 6 March 2017
© Author(s) 2017. CC-BY 3.0 License.

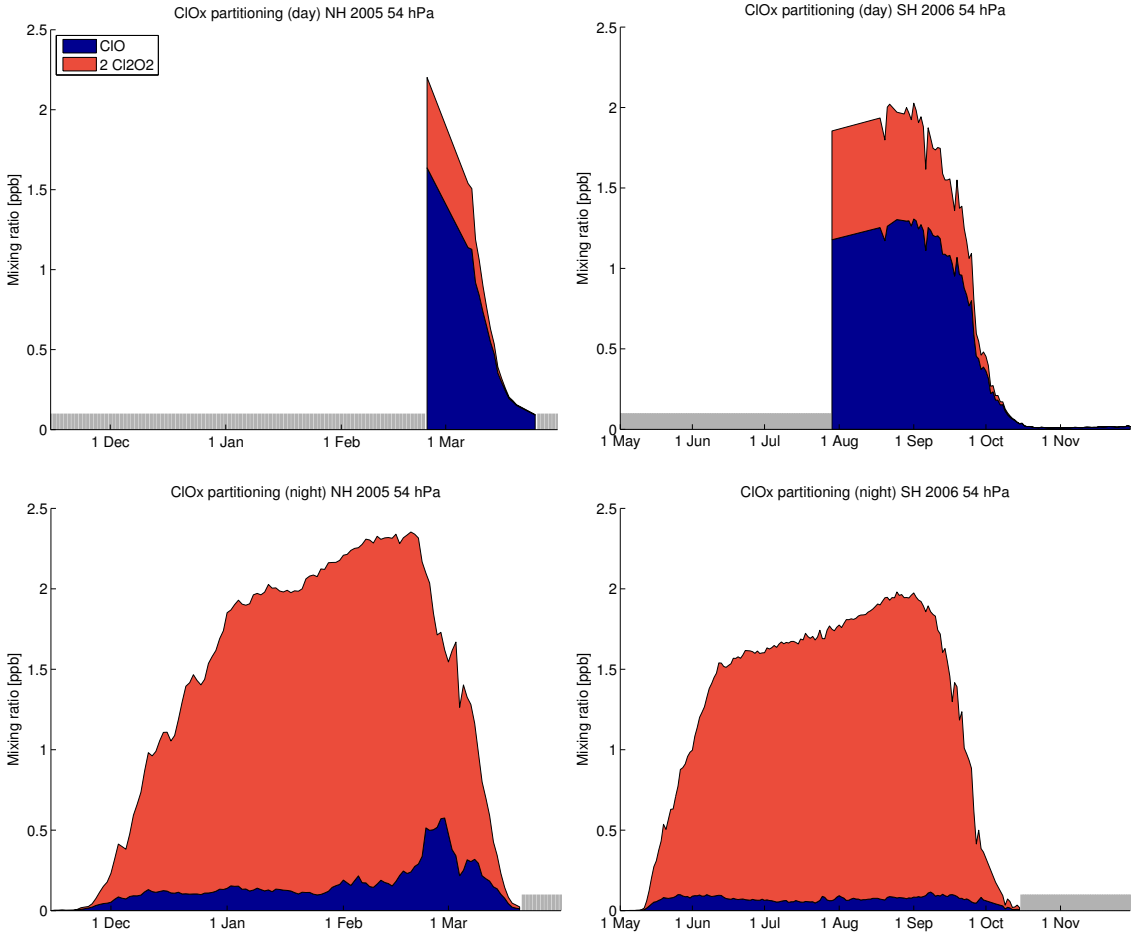

Figure 12. Vortex-averaged partitioning of ClO_x for the Arctic winter 2004/2005 (left) and the Antarctic winter 2006 (right) at 54 hPa. Top row: Daytime averages (parts of the vortex where the solar zenith angle is smaller than 80°). Bottom row: Nighttime averages (parts of the vortex where the solar zenith angle is larger than 100°). Days without sufficient data for averaging are not shown (grey bars).

Atmos. Chem. Phys. Discuss., doi:10.5194/acp-2017-66, 2017
Manuscript under review for journal Atmos. Chem. Phys.
Discussion started: 6 March 2017
© Author(s) 2017. CC-BY 3.0 License.

removed by heterogeneous reactions on polar stratospheric clouds and active chlorine is produced. When sunlight returns, this is followed by a phase of competition between HCl removal by heterogeneous reactions and deactivation of ClO_x into HCl by gas-phase reactions (most pronounced in August in the southern hemisphere). In the southern hemisphere, this is followed by a phase of deactivation of active chlorine into HCl by the $Cl + CH_4$ reaction in September to October. Finally, when sunlight comes back, the gas-phase loss reaction $HCl + OH$ becomes important and competes with the production by $Cl + CH_4$. In the southern hemisphere, HCl is near equilibrium during this time, while in the northern hemisphere, chlorine that was initially deactivated into $ClONO_2$ is slowly transformed into HCl.

HCl loss (chlorine activation)

The most important heterogeneous loss reaction for HCl is

$$ClONO_2 + HCl \rightarrow Cl_2 + HNO_3 \quad \text{(R4)}$$

Another heterogeneous activation channel for HCl is

$$HOCl + HCl \rightarrow Cl_2 + H_2O. \quad \text{(R23)}$$

While this reaction plays a smaller role in the northern hemisphere, the reaction is important in the southern hemisphere in the months August and September. In the southern hemisphere, the $HOCl + HCl$ reaction accounts for about 70 % of the HCl activation by heterogeneous reactions and in the northern hemisphere it accounts for about 30 %. HOCl only exists in significant amounts when chlorine is activated. In the southern hemisphere, this causes a shift from activation by $ClONO_2 + HCl$ in early winter to activation dominated by $HOCl + HCl$ later.

The only other reaction that removes HCl in relevant quantities is the gas-phase reaction with OH, which is only important under sunlit conditions:

$$HCl + OH \rightarrow H_2O + Cl. \quad \text{(R17)}$$

In the northern hemisphere, the reaction is relevant in late winter (March). For the southern hemisphere, the reaction is relevant in October and later.

HCl production (chlorine deactivation)

HCl is only produced by reactions that are indirectly dependent on sunlight. Deactivation of active chlorine occurs mainly into HCl in the southern hemisphere but predominantly into $ClONO_2$ in the northern hemisphere. The reason for this is that deactivation into $ClONO_2$ is hindered in the southern hemisphere by strong denitrification (absence of NO_2), while normally it would be the preferred pathway of deactivation.

In the long term, the partitioning of HCl and $ClONO_2$ in spring and summer favors HCl. This can be seen in the fact that in the northern hemisphere, HCl is produced from $ClONO_2$ in spring after ClO_x has been deactivated into $ClONO_2$ some time

Atmos. Chem. Phys. Discuss., doi:10.5194/acp-2017-66, 2017
Manuscript under review for journal Atmos. Chem. Phys.
Discussion started: 6 March 2017
© Author(s) 2017. CC-BY 3.0 License.

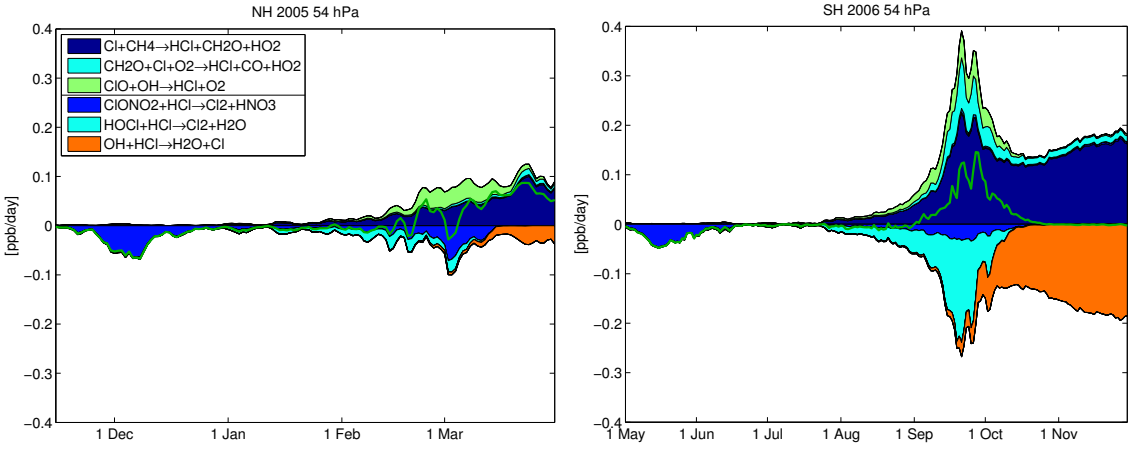

Figure 13. Vortex-averaged chemical reaction rates of reactions involving HCl for the Arctic winter 2004/2005 (left) and the Antarctic winter 2006 (right) at 54 hPa. Production reactions are shown positive and are separated by a line in the legend from the loss reactions, which are shown negative. The net change of HCl is shown as a green line. Reactions with rates which cannot be distinguished from the zero line at plot resolution are not shown.

earlier (see also section 4.3.3 and Figure 17), while in the southern hemisphere, active chlorine is deactivated mainly into HCl. The chemical change rates of both HCl and $ClONO_2$ decrease to zero in November in the southern hemisphere. The reaction

$$Cl + CH_4 \rightarrow HCl + CH_3 \quad \text{(R33)}$$

is the main production reaction for HCl in both hemispheres. In addition, it is responsible for deactivation under ozone hole conditions in the southern hemisphere. The reaction

$$ClO + OH \rightarrow HCl + O_2 \quad \text{(R20)}$$

becomes similar in importance to $Cl + CH_4$ as a production process for HCl around late February in the northern hemisphere, and plays a smaller role earlier and later in winter. In the southern hemisphere, the reaction is not negligible around September and October. The reaction is responsible for a part of the chlorine deactivation in both hemispheres. The reaction $ClO + OH$ has two product channels. The channel into HCl yields about $\approx 8\,\%$ of the products (the other channel is into ClO).

The role of Cl in HCl production

The rate of the $Cl + CH_4$ reaction is proportional to the mixing ratio of Cl. Figure 14 shows the mixing ratio of Cl for both hemispheres. Figure 15 shows that Cl is determined by the two source reactions

$$Cl_2O_2 + h\nu \rightarrow 2\,Cl + O_2 \quad \text{(R31)}$$

$$ClO + NO \rightarrow Cl + NO_2 \quad \text{(R7)}$$

Atmos. Chem. Phys. Discuss., doi:10.5194/acp-2017-66, 2017
Manuscript under review for journal Atmos. Chem. Phys.
Discussion started: 6 March 2017
© Author(s) 2017. CC-BY 3.0 License.

Atmospheric Chemistry and Physics Discussions

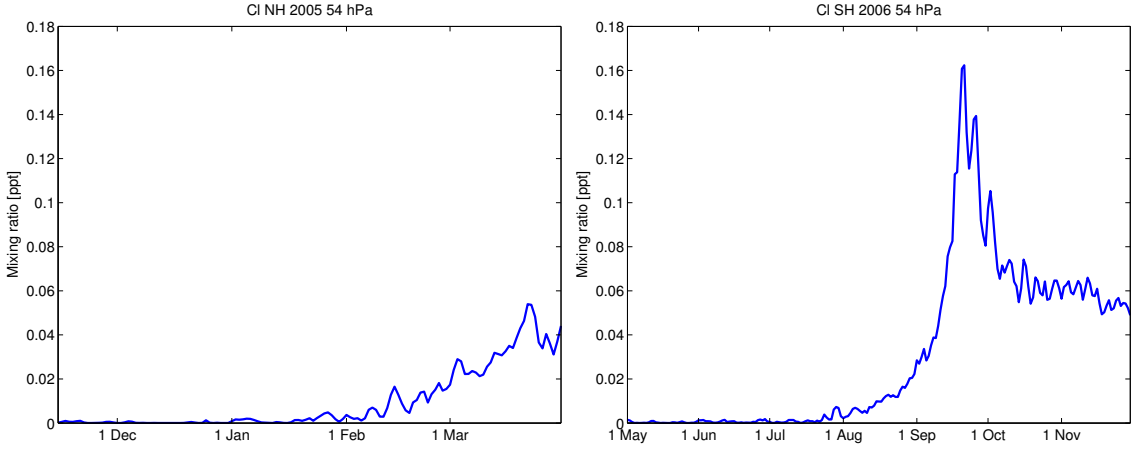

Figure 14. Vortex-averaged Cl mixing ratios for the Arctic winter 2004/2005 and the Antarctic winter 2006 at 54 hPa.

and a reaction that removes Cl

$$\mathrm{Cl} + \mathrm{O_3} \rightarrow \mathrm{ClO} + \mathrm{O_2}. \tag{R29}$$

Reaction R31 is coupled to the catalytic ClO dimer cycle. Cl levels are considerably higher in the southern hemisphere due to a lack of ozone, which hinders the recombination to ClO. This favors the deactivation of active chlorine over the $\mathrm{Cl} + \mathrm{CH_4}$ reaction. Cl shows a very distinct behaviour in the southern hemisphere. It does not just increase with the amount of sunlight, but shows a peak in September, followed by a near constant plateau. This curve shape is approximately repeated in the curves of the reaction rate of the $\mathrm{Cl} + \mathrm{CH_4}$ reaction, since $\mathrm{CH_4}$ is relatively constant. Figure 15 shows that the peak in Cl mixing ratios in the southern hemisphere is related to reaction R31, i.e. the catalytic ozone destruction. In contrast, the plateau is related to the $\mathrm{NO_x}$ reaction R7 (see also Wayne et al., 1995, p. 2836).

4.3.3 Reservoir $\mathrm{ClONO_2}$

Figure 16 shows the reaction rates of the most important reactions changing $\mathrm{ClONO_2}$. As discussed in section 4.1, the gross change rates of $\mathrm{ClONO_2}$ are dominated by a near equilibrium between the reactions

$$\mathrm{ClONO_2} + h\nu \rightarrow \mathrm{Cl} + \mathrm{NO_3} \tag{R10}$$

$$\rightarrow \mathrm{ClO} + \mathrm{NO_2} \tag{R11}$$

and

$$\mathrm{ClO} + \mathrm{NO_2} + \mathrm{M} \rightarrow \mathrm{ClONO_2} + \mathrm{M} \tag{R12}$$

under sunlit conditions. Net changes of $\mathrm{ClONO_2}$ are induced by changes in $\mathrm{NO_x}$ which shift the equilibrium.

Atmos. Chem. Phys. Discuss., doi:10.5194/acp-2017-66, 2017
Manuscript under review for journal Atmos. Chem. Phys.
Discussion started: 6 March 2017
© Author(s) 2017. CC-BY 3.0 License.

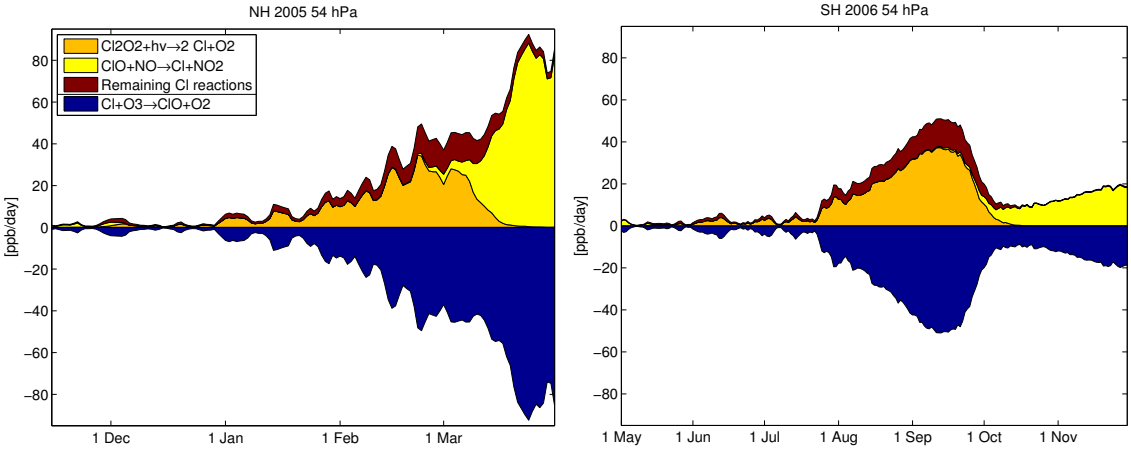

Figure 15. Vortex-averaged chemical reaction rates of reactions involving Cl for the Arctic winter 2004/2005 (left) and the Antarctic winter 2006 (right) at 54 hPa. Production reactions are shown positive and are separated by a line in the legend from the loss reactions, which are shown negative.

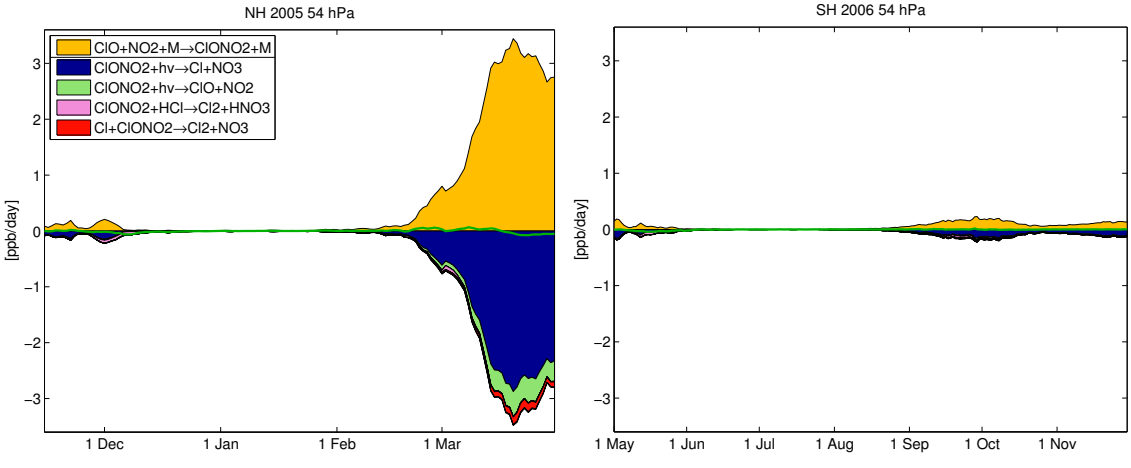

Figure 16. Vortex-averaged chemical reaction rates involving $ClONO_2$ for the Arctic winter 2004/2005 and the Antarctic winter 2006 at 54 hPa. Production reactions are shown positive and are separated by a line in the legend from the loss reactions, which are shown negative. The net change of $ClONO_2$ is shown as a green line. Reactions with rates which cannot be distinguished from the zero line at plot resolution are not shown.

Atmos. Chem. Phys. Discuss., doi:10.5194/acp-2017-66, 2017
Manuscript under review for journal Atmos. Chem. Phys.
Discussion started: 6 March 2017
© Author(s) 2017. CC-BY 3.0 License.

Atmospheric Chemistry and Physics Discussions

The net change of $ClONO_2$ is one order of magnitude smaller than the gross rates. Figure 17 shows the net effect of R10–R12 (yellow area) and all other reactions that play a role in changing $ClONO_2$. These reactions, which are all loss reactions, remove $ClONO_2$ either by heterogeneous reactions or gas-phase reactions of $ClONO_2$ with a radical. The most important heterogeneous reaction is the same as for HCl

$$ClONO_2 + HCl \rightarrow Cl_2 + HNO_3. \quad \text{(R4)}$$

The reactions of $ClONO_2$ with a radical are of the type

$$ClONO_2 + X \rightarrow XCl + NO_3 \quad \text{(R34)}$$

where X is $X = O, Cl, OH$. The reaction with Cl is the dominating reaction.

In early winter in the polar night (December in the northern hemisphere, May and June in the southern hemisphere), the loss of $ClONO_2$ by heterogeneous reactions is dominating, leading to the activation of chlorine. After the complete depletion of $ClONO_2$, this is followed by a phase with only small production and loss, due to near-zero levels of both NO_x and $ClONO_2$. The peak in production in early spring in the northern hemisphere (end of February and beginning of March) is caused by the net production of extended NO_x from HNO_3 and is the main deactivation pathway for active chlorine in the northern hemisphere. Then, $ClONO_2$ is out of equilibrium and more $ClONO_2$ is produced by $ClO + NO_2$ than is lost by photolysis. In the southern hemisphere, the rates are much lower due to the strongly denitrified conditions. In late March, $ClONO_2$ is lost in the northern hemisphere and finally converted to HCl, which is the favored reservoir under summer conditions. In the southern hemisphere, rates are low in late October and November, since the deactivation already occured into HCl.

4.4 Bromine species

Sources of inorganic bromine, which has both natural and anthropogenic sources, are mainly halons and methyl bromide, but also some short-lived species (e.g. WMO, 2011; Montzka, 2012). Inorganic bromine (Br_y) levels in the stratosphere are about 20 ppt at maximum (e.g. WMO, 2011), with marginally lower levels in the altitude range considered here. Bromine chemistry is still somewhat uncertain due to uncertainties in the reaction constants (Sander et al., 2011; von Hobe and Stroh, 2012).

Atomic bromine is released from the source gases mainly by photolysis. Under sunlit conditions, it is in equilibrium with BrO. The relevant reactions are

$$Br + O_3 \rightarrow BrO + O_2 \quad \text{(R35)}$$

$$BrO + h\nu \rightarrow Br + O \quad \text{(R36)}$$

$$BrO + NO \rightarrow NO_2 + Br \quad \text{(R37)}$$

Atmos. Chem. Phys. Discuss., doi:10.5194/acp-2017-66, 2017
Manuscript under review for journal Atmos. Chem. Phys.
Discussion started: 6 March 2017
© Author(s) 2017. CC-BY 3.0 License.

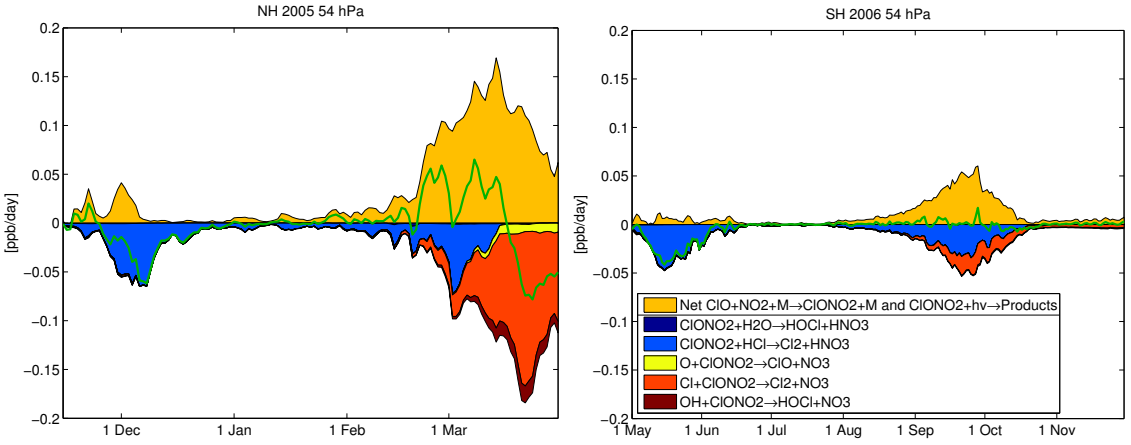

Figure 17. Vortex-averaged chemical reaction rates involving $ClONO_2$ for the Arctic winter 2004/2005 and the Antarctic winter 2006 at 54 hPa. In contrast to Figure 16, the net production rate of the fast cycle $ClONO_2 + h\nu \rightarrow Products / ClO + NO_2 + M \rightarrow ClONO_2 + M$ is shown. This cycle is separated by a line in the legend from the loss reactions. The green line shows the net change of $ClONO_2$ by chemistry. Reactions with rates which cannot be distinguished from the zero line at plot resolution are not shown.

$$BrO + ClO \rightarrow Br + Cl + O_2. \quad \text{(R38)}$$

Reactions R35 and R38 are directly involved in the ClO–BrO cycle, see section 4.5.

Figure 18 shows the partitioning between the various inorganic bromine species. Bromine is mostly present in the form of HOBr and $BrONO_2$ at night before chlorine activation starts. In contrast to the less reactive chlorine, these are not real reservoir gases, since they easily photolyze into Br and react further to BrO during daytime, which gives bromine a great potential to destroy ozone despite the low mixing ratios (e.g. Lary, 1996). BrO is a dominant species during daytime (e.g. Lary, 1996), except in October and November in the southern hemisphere, when the reaction $Br + O_3$ is hindered by the low ozone levels and Br mixing ratios are significant. Heterogeneous reactions play only a minor role and are not needed for activation (e.g. Lary et al., 1996; Wayne et al., 1995). As long as chlorine is activated, almost all bromine is in the form of BrCl at night (e.g. Lary et al., 1996; von Hobe and Stroh, 2012). BrCl is produced by the reaction

$$BrO + ClO \rightarrow BrCl + O_2. \quad \text{(R39)}$$

During daytime, most of this BrCl is transformed to Br by photolysis

$$BrCl + h\nu \rightarrow Br + Cl \quad \text{(R40)}$$

followed by transformation to BrO by reaction R35.

Atmos. Chem. Phys. Discuss., doi:10.5194/acp-2017-66, 2017
Manuscript under review for journal Atmos. Chem. Phys.
Discussion started: 6 March 2017
© Author(s) 2017. CC-BY 3.0 License.

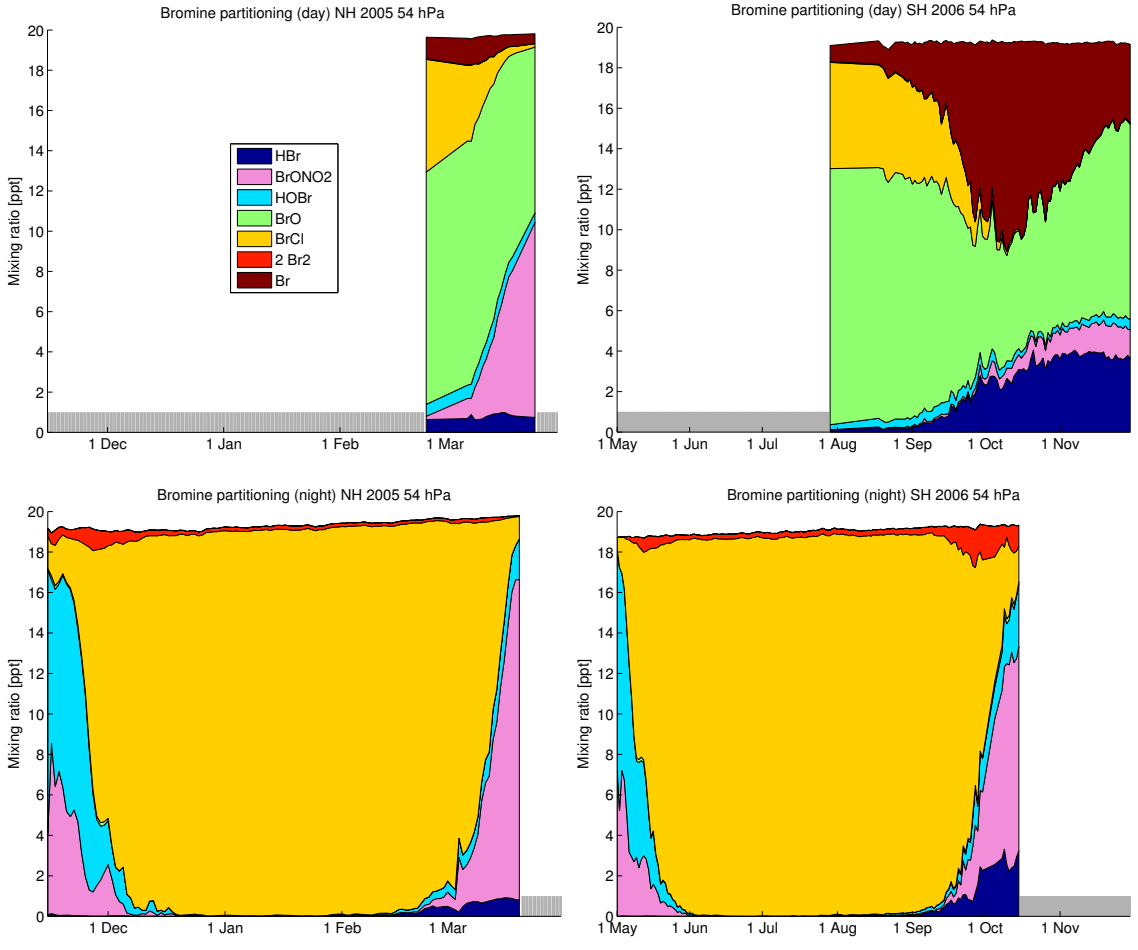

Figure 18. Vortex-averaged partitioning of inorganic bromine species for the Arctic winter 2004/2005 (left) and the Antarctic winter 2006 (right) at 54 hPa. Top row: Daytime averages (parts of the vortex where the solar zenith angle is smaller than 80°). Bottom row: Nighttime averages (parts of the vortex where the solar zenith angle is larger than 100°). Days without sufficient data for averaging are not shown (grey bars).

Atmos. Chem. Phys. Discuss., doi:10.5194/acp-2017-66, 2017
Manuscript under review for journal Atmos. Chem. Phys.
Discussion started: 6 March 2017
© Author(s) 2017. CC-BY 3.0 License.

Atmospheric Chemistry and Physics Discussions

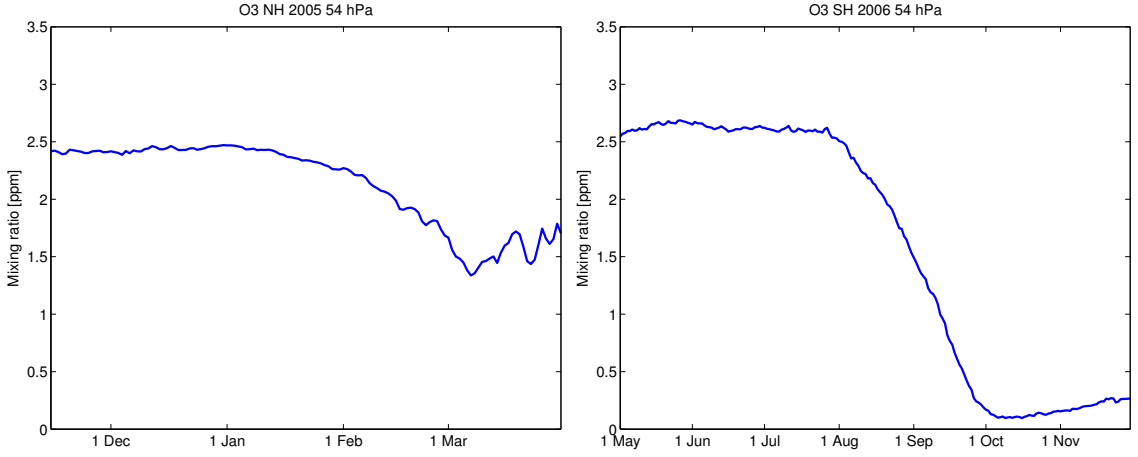

Figure 19. Ozone mixing ratios for the Arctic winter 2004/2005 and the Antarctic winter 2006 at 54 hPa.

4.5 Oxygen species

Figure 19 shows the vortex-averaged mixing ratios of ozone for the northern and southern hemisphere. Ozone stays relatively constant at values between 1.5 ppm and 2.5 ppm in the northern hemisphere, since the change by ozone depletion is nearly cancelled by transport of air rich in ozone from above and over the vortex edge. In contrast, ozone values decrease from 2.5 ppm to less than 0.5 ppm in the southern hemisphere, both due to weaker transport and larger ozone depletion.

O_3 is in a very fast equilibrium with O. The dominant cycle is part of the well-known Chapman chemistry (Chapman, 1930)

$$O_3 + h\nu \rightarrow O + O_2 \tag{R41}$$

$$O + O_2 + M \rightarrow O_3 + M. \tag{R42}$$

We follow the usual convention here to treat O_3 and O together as odd oxygen O_x (e.g. Brasseur and Solomon, 2005; Solomon, 1999). Since O mixing ratios are low, the chemical rate of change of O_x is nearly the same as the rate of change of ozone.

Odd oxygen is destroyed by several catalytic cycles. It is well known (e.g. Solomon, 1999) that the two dominating cycles in anthropogenic polar ozone depletion by halogens are the ClO dimer cycle (first proposed by Molina and Molina, 1987)

$$2\,(Cl + O_3 \rightarrow ClO + O_2) \tag{R29}$$

$$ClO + ClO + M \rightarrow Cl_2O_2 + M \tag{R30}$$

$$Cl_2O_2 + h\nu \xrightarrow{M} 2\,Cl + O_2 \tag{R31}$$

$$2\,O_3 \rightarrow 3\,O_2$$

Atmos. Chem. Phys. Discuss., doi:10.5194/acp-2017-66, 2017
Manuscript under review for journal Atmos. Chem. Phys.
Discussion started: 6 March 2017
© Author(s) 2017. CC-BY 3.0 License.

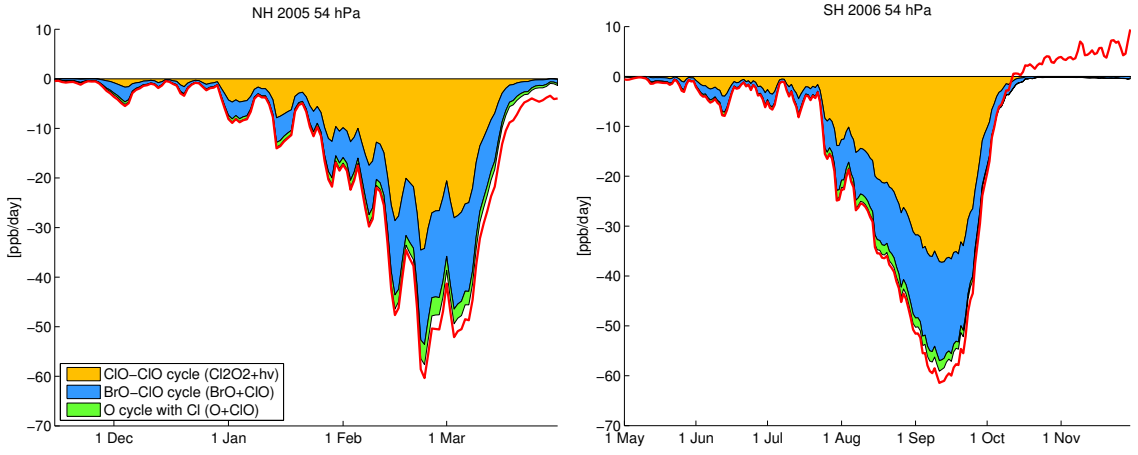

Figure 20. Vortex-averaged net chemical loss of odd oxygen by different catalytic cycles. The red line shows the net chemical change rate of ozone. The contribution of the different cycles is shown by the reaction rates of their rate limiting step. Only the three most important cycles are shown, the contribution of other cycles is negligible. The ozone increase in the right panel is caused by the $O_2 + h\nu$ reaction.

and the ClO–BrO cycle (first proposed by McElroy et al., 1986)

$$\mathrm{Cl} + \mathrm{O_3} \rightarrow \mathrm{ClO} + \mathrm{O_2} \qquad \text{(R29)}$$

$$\mathrm{Br} + \mathrm{O_3} \rightarrow \mathrm{BrO} + \mathrm{O_2} \qquad \text{(R35)}$$

$$\mathrm{BrO} + \mathrm{ClO} \xrightarrow{\mathrm{M}} \mathrm{Br} + \mathrm{Cl} + \mathrm{O_2} \qquad \text{(R38)}$$

$$2\,\mathrm{O_3} \rightarrow 3\,\mathrm{O_2}.$$

The ClO dimer cycle is able to work, because the Cl_2O_2 photolysis, which produces Cl and not ClO, is fast compared to the competing Cl_2O_2 loss reaction $Cl_2O_2 + M$ (Wayne et al., 1995, p. 2836). The uncertainty of the rate constant of the Cl_2O_2 photolysis R31 and the rate constant of the $BrO + ClO$ reaction R38 are two of the parameters which produce the largest uncertainties with respect to ozone loss in models, although much of the uncertainty in the photolysis has been resolved recently (Kawa et al., 2009; von Hobe and Stroh, 2012).

Figure 20 shows the contribution of the different catalytic cycles to the net chemical rate of change of ozone. For this purpose, the reaction rates of the rate limiting step of the reaction cycles have been used. This is possible here without ambiguities, since all rate limiting reactions are only involved in one cycle.

As long as appreciable amounts of ClO exist (January to February in the northern hemisphere, June to September in the southern hemisphere), the ClO–ClO cycle contributes about 50 % to the net ozone loss and the ClO–BrO cycle contributes

Atmos. Chem. Phys. Discuss., doi:10.5194/acp-2017-66, 2017
Manuscript under review for journal Atmos. Chem. Phys.
Discussion started: 6 March 2017
© Author(s) 2017. CC-BY 3.0 License.

Atmospheric Chemistry and Physics Discussions

about 40 % (see also Grenfell et al., 2006, for case studies of the partitioning). Loss cycles of the form

$$\begin{aligned} &\mathrm{X} + \mathrm{O_3} \rightarrow \mathrm{XO} + \mathrm{O_2} \\ &\underline{\mathrm{XO} + \mathrm{O} \rightarrow \mathrm{X} + \mathrm{O_2}} \\ &\mathrm{O} + \mathrm{O_3} \rightarrow \mathrm{O_2} + \mathrm{O_2} \end{aligned}$$

where $\mathrm{X} = \mathrm{OH}, \mathrm{H}, \mathrm{NO}, \mathrm{Cl}, \mathrm{Br}$, which dominate in most latitudes and seasons, only play a minor role in the polar lower stratosphere due to the relatively low production of atomic oxygen by photolysis (e.g. von Hobe and Stroh, 2012).

The most important null cycle acting on odd oxygen apart from reactions R41 and R42 is the nitrogen cycle

$$\begin{aligned} &\mathrm{O_3} + \mathrm{NO} \rightarrow \mathrm{NO_2} + \mathrm{O_2} \qquad \text{(R6)} \\ &\underline{\mathrm{NO_2} + h\nu \rightarrow \mathrm{NO} + \mathrm{O} \qquad \text{(R8)}} \\ &\mathrm{O_3} \rightarrow \mathrm{O_2} + \mathrm{O}. \end{aligned}$$

5 Conclusions

We have given a quantitative analysis of the reactions involved in polar ozone depletion in the stratosphere. For clarity, this study focuses on vortex averages in a layer around 54 hPa. The reactions and reaction cycles involved in polar ozone depletion are well known, but quantitative estimates of the partitioning of the chemical families or the importance of single reactions and reaction cycles are rare. To our knowledge, this is the first comprehensive study providing quantitative results averaged over the polar vortex under conditions perturbed by heterogeneous chemistry. The main aim of this study is to quantify numbers for the partitioning of $\mathrm{HO_x}$, $\mathrm{NO_x}$ and $\mathrm{ClO_x}$, the relative importance of production and loss reactions and the timing of the reactions. Some selected findings are:

- The ClO dimer cycle contributes about 50% to the vortex-averaged ozone loss at 54 hPa in both hemispheres, while the ClO–BrO cycle contributes about 40%.
- In the southern hemisphere, there is a clear shift from chlorine activation by the $\mathrm{ClONO_2} + \mathrm{HCl}$ reaction in early winter to activation by the $\mathrm{HOCl} + \mathrm{HCl}$ reaction later in winter. $\mathrm{HOCl} + \mathrm{HCl}$ accounts for about 70% of the activation of HCl in the southern hemisphere, while it accounts for 30% of the activation in the northern hemisphere.
- $\mathrm{ClO_x}$ peaks at 2.0–2.5 ppb. About 70% of $\mathrm{ClO_x}$ is present as ClO during daytime at 54 hPa.
- $\mathrm{HO_x}$ levels peak at 4 ppt. $\mathrm{HO_x}$ is mainly produced from $\mathrm{CH_4}$ oxidation in the southern hemisphere, while in the northern hemisphere, production by $\mathrm{HNO_3}$, $\mathrm{CH_4}$ and $\mathrm{H_2O}$ play comparable roles. The partitioning between OH and $\mathrm{HO_2}$ results in 20%–40% OH in the southern hemisphere and in 10%–20% OH in the northern hemisphere.
- $\mathrm{NO_x}$ levels are smaller than 2 ppb in the northern hemisphere and smaller than 0.75 ppb in the southern hemisphere due to the denitrified conditions there. The partitioning between NO and $\mathrm{NO_2}$ during daytime results in 80 %–90 % NO in

Atmos. Chem. Phys. Discuss., doi:10.5194/acp-2017-66, 2017
Manuscript under review for journal Atmos. Chem. Phys.
Discussion started: 6 March 2017
© Author(s) 2017. CC-BY 3.0 License.

Atmospheric Chemistry and Physics Discussions

the southern hemisphere and 20 %–40 % NO in the northern hemisphere. The higher NO levels are caused by the much lower ozone levels in the southern hemisphere.

- 60%–80% of the production of NO_x in spring are caused by the $HNO_3 + OH$ reaction, the remainder is caused by the $HNO_3 + h\nu$ reaction. Deactivation of ClO_x by the formation of $ClONO_2$ in the northern hemisphere is caused by a shift in the fast equilibrium between ClO, NO_2 and $ClONO_2$, which in turn is caused by the production of NO_x.

Results of this study are extensively used in a companion paper (Wohltmann et al., in preparation) to develop a fast model for polar ozone chemistry.

Appendix A: Model validation: HCl discrepancy between model and measurements

It is desirable that the results of the ATLAS model agree well with observations to increase the confidence in the model results for minor species and reaction rates which cannot be backed up by observations. It is out of the scope of this study to give a comprehensive model validation against observations, and the reader is referred to Wohltmann et al. (2010) and Wohltmann et al. (2013) for a detailed validation. We will show only some selected results here. The focus is on a prominent disagreement between modeled mixing ratios of HCl and observations.

Figure 21 and 22 show a comparison of the vortex-averaged mixing ratios of some important species (ozone, water vapor, HNO_3 and HCl, blue and black lines) with corresponding vortex averages measured by the MLS satellite instrument (red circles). Note that the vortex averages do not take into account the vortex tracer criterion, as in the main part of the paper, to facilitate comparison with MLS. The blue lines denote the runs actually used in this paper, and the black lines denote an earlier version of the model runs. It is obvious that the earlier version significantly overestimates HCl, a behaviour also observed in other models (Wegner et al., 2013). Apart from this, the agreement of model and observations for other species like ozone, water vapour or HNO_3 is quite satisfactory. The reason for this discrepancy is unknown, but several solutions are possible:

- The initial amount of $ClONO_2$ in the model is underestimated, which hinders the $HCl + ClONO_2$ reaction. This is unlikely, since it is not supported by measurements of $ClONO_2$ by ACE-FTS (not shown here) and would require increasing the $ClONO_2$ mixing ratios by more than 100 %.

- Less NO_x is transported over the vortex edge in the model compared to the real atmosphere, which impedes the reformation of $ClONO_2$ and HCl depletion over the $HCl + ClONO_2$ reaction. While this cannot be excluded, the good agreement of most other species with measurements, including the tracer N_2O (not shown), suggests that this option is unlikely.

- HCl is taken up in PSCs and sediments out of the observed layer. This is not supported by either the temporal or the spatial evolution of HCl.

- An unknown heterogeneous reaction is depleting HCl. This cannot be excluded, but some boundary conditions need to be fulfilled, e.g. the reaction needs to involve HCl and it must not change the mixing ratios of observed species too much.

Atmos. Chem. Phys. Discuss., doi:10.5194/acp-2017-66, 2017
Manuscript under review for journal Atmos. Chem. Phys.
Discussion started: 6 March 2017
© Author(s) 2017. CC-BY 3.0 License.

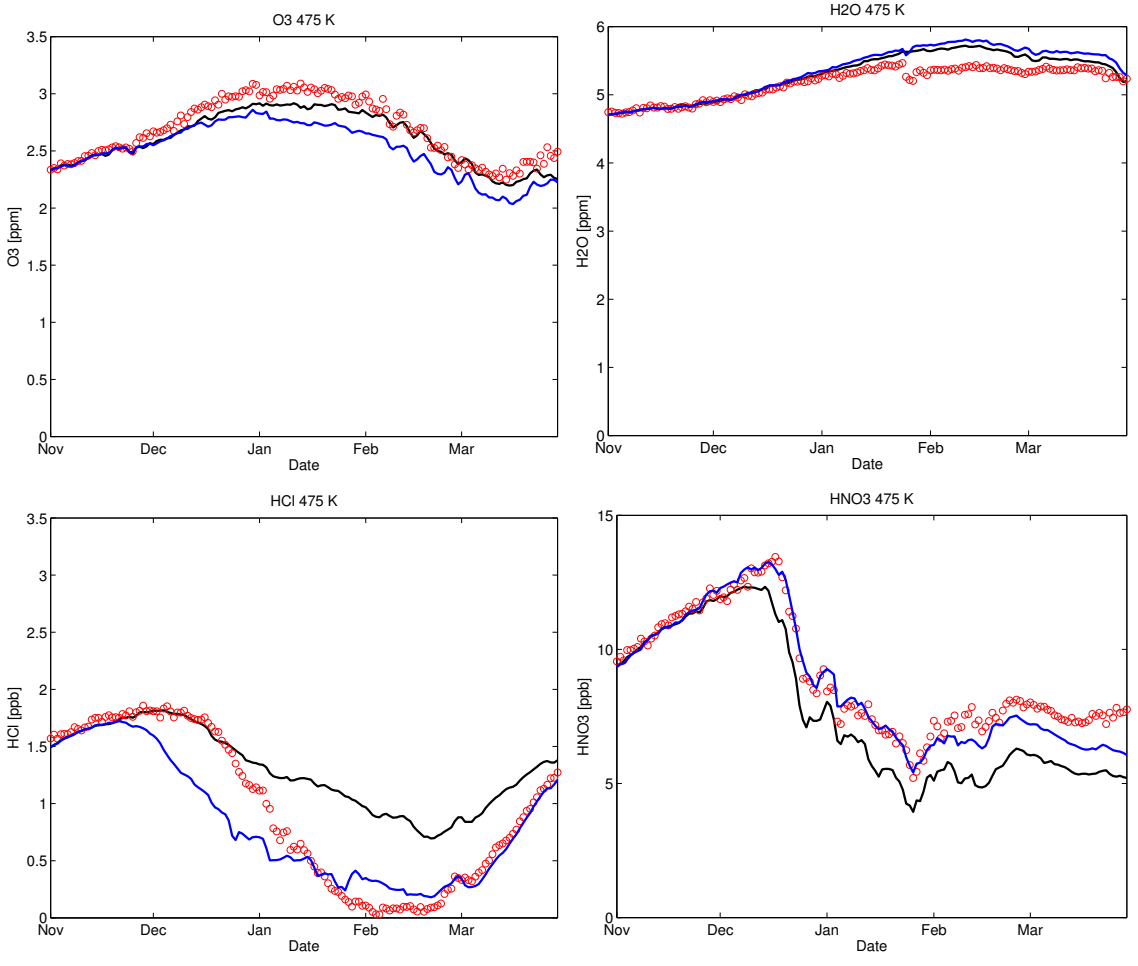

Figure 21. Vortex-averaged mixing ratios of O_3, H_2O, HCl and HNO_3 for the Arctic winter 2004/2005. The red dots show MLS satellite measurements, the blue lines show the ATLAS runs used in this paper and the black line shows the original runs which are not empirically corrected for the HCl discrepancy.

Atmos. Chem. Phys. Discuss., doi:10.5194/acp-2017-66, 2017
Manuscript under review for journal Atmos. Chem. Phys.
Discussion started: 6 March 2017
© Author(s) 2017. CC-BY 3.0 License.

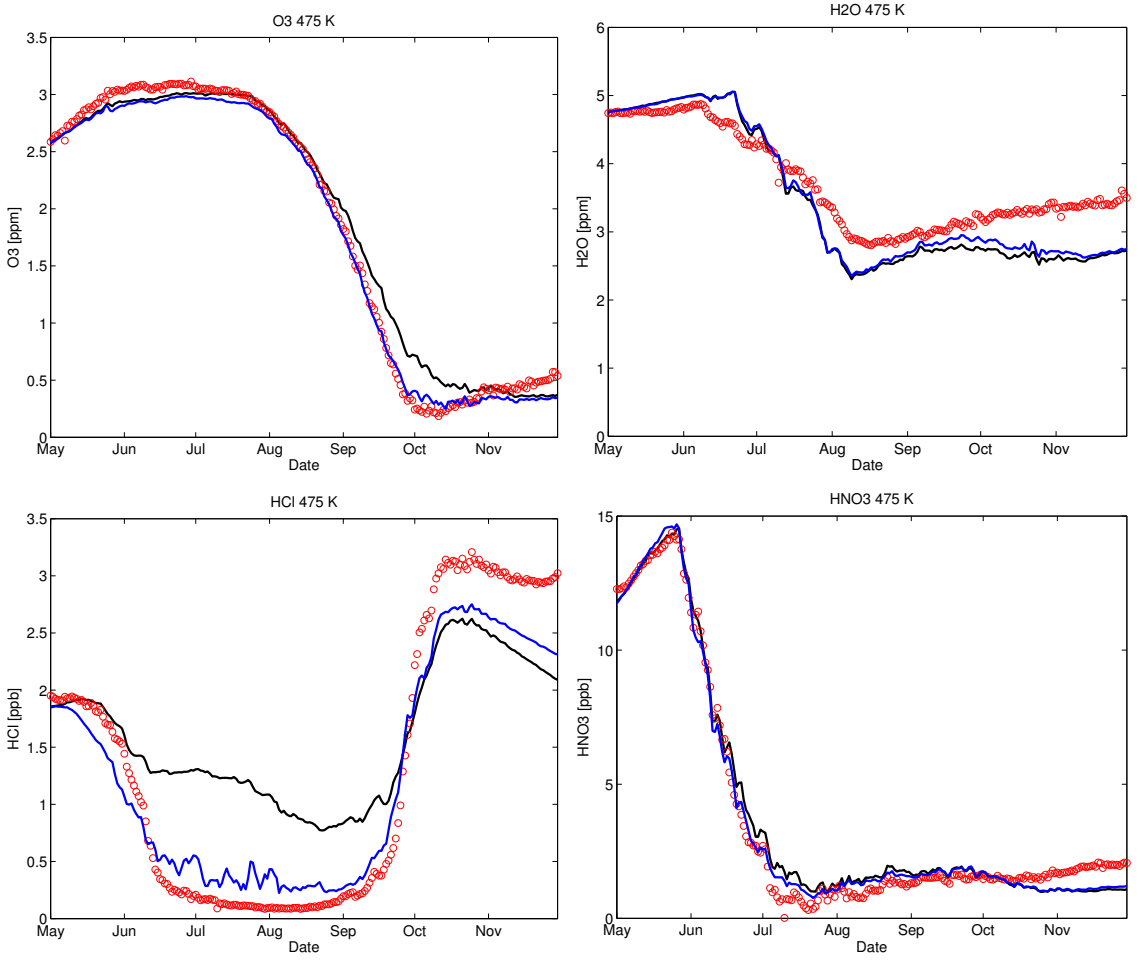

Figure 22. Comparison of vortex-averaged mixing ratios for the Antarctic winter 2006

– The solubility of HCl in STS droplets is underestimated. This is a promising possibility, but it requires changes to the solubility that are above the stated uncertainties of the solubility parameterization by Luo et al. (1995) that is used in the model.

Since there is not enough evidence to narrow down this list to a likely candidate, we decided on an empirical approach: We introduced a temperature offset for the calculation of the Henry constant of HCl and changed the offset until we obtained a good agreement of measured and modeled HCl, which was the case for an offset of $-5\,\mathrm{K}$. The effect of the changed Henry constant is twofold: First, it increases the amount of HCl dissolved in STS droplets. Second, it increases the rates of the heterogeneous reactions (even if only small amounts of HCl are dissolved) by changing the γ values. The HCl mixing ratios of the model runs with the changed Henry constant agree well with the satellite measurements for the southern hemisphere and the northern hemisphere after beginning of January, but a discrepany remains in December.

Atmos. Chem. Phys. Discuss., doi:10.5194/acp-2017-66, 2017
Manuscript under review for journal Atmos. Chem. Phys.
Discussion started: 6 March 2017
© Author(s) 2017. CC-BY 3.0 License.

Acknowledgements. This work was supported by the BMBF under the FAST-O3 project in the MiKliP framework programme (FKZ 01LP1137A) and in the MiKliP II programme (FKZ 01LP1517E). This research has received funding from the European Community's Seventh Framework Programme (FP7/2007–2013) under grant agreement no. 603557. We thank ECMWF for providing reanalysis data.

Atmos. Chem. Phys. Discuss., doi:10.5194/acp-2017-66, 2017
Manuscript under review for journal Atmos. Chem. Phys.
Discussion started: 6 March 2017
© Author(s) 2017. CC-BY 3.0 License.

Atmospheric Chemistry and Physics Discussions

References

Brasseur, G. and Solomon, S.: Aeronomy of the Middle Atmosphere, D. Reidel Publishing Company, Dordrecht, 2005.

Brasseur, G., Orlando, J. J., and Tyndall, G. S., eds.: Atmospheric Chemistry and Global Change, Oxford University Press, New York, Oxford, 1999.

Chapman, S.: A theory of upper-atmospheric ozone, Mem. Roy. Soc., 3, 103–125, 1930.

Cohen, R. C., Wennberg, P. O., Stimpfle, M., Koplow, J., Anderson, J. G., Fahey, D. W., Woodbridge, E. L., Keim, E. R., Gao, R., Proffitt, M. H., Loewenstein, M., and Chan, K. R.: Are models of catalytic removal of O_3 by HO_x accurate? Constraints from in situ measurements of the OH to HO_2 ratio, Geophys. Res. Lett., 21, 2539–2542, 1994.

Dee, D. P., Uppala, S. M., Simmons, A. J., Berrisford, P., Poli, P., Kobayashi, S., Andrae, U., Balmaseda, M. A., Balsamo, G., Bauer, P., Bechtold, P., Beljaars, A. C. M., van de Berg, L., Bidlot, J., Bormann, N., Delsol, C., Dragani, R., Fuentes, M., Geer, A. J., Haimberger, L., Healy, S. B., Hersbach, H., Hólm, E. V., Isaksen, L., Kållberg, P., Köhler, M., Matricardi, M., McNally, A. P., Monge-Sanz, B. M., Morcrette, J.-J., Park, B.-K., Peubey, C., de Rosnay, P., Tavolato, C., Thépaut, J.-N., and Vitart, F.: The ERA-Interim reanalysis: configuration and performance of the data assimilation system, Q. J. R. Meteorol. Soc., 137, 553–597, 2011.

Grenfell, J. L., Lehmann, R., Mieth, P., Langematz, U., and Steil, B.: Chemical reaction pathways affecting stratospheric and mesospheric ozone, J. Geophys. Res., 111, D17311, doi:10.1029/2004JD005713, 2006.

Grooß, J.-U. and Russell III, J. M.: Technical note: A stratospheric climatology for O_3, H_2O, CH_4, NO_x, HCl and HF derived from HALOE measurements, Atmos. Chem. Phys., 5, 2797–2807, 2005.

Grooß, J.-U., Günther, G., Konopka, P., Müller, R., McKenna, D. S., Stroh, F., Vogel, B., Engel, A., Müller, M., Hoppel, K., Bevilacqua, R., Richard, E., Webster, C. R., Elkins, J. W., Hurst, D. F., Romashkin, P. A., and Baumgardner, D. G.: Simulation of ozone depletion in spring 2000 with the Chemical Lagrangian Model of the Stratosphere (CLaMS), J. Geophys. Res., 107, 8295, doi:10.1029/2001JD000456, 2002.

Hanisco, T. F.: Stratospheric chemistry and composition / HO_x, in: Encyclopedia of Atmospheric Sciences, edited by Holton, J. R., Curry, J. A., and Pyle, J. A., vol. 5, pp. 2174–2180, Academic Press, Elsevier, 2003.

Kawa, S. R., Stolarski, R. S., Newman, P. A., Douglass, A. R., Rex, M., Hofmann, D. J., Santee, M. L., and Frieler, K.: Sensitivity of polar stratospheric ozone loss to uncertainties in chemical reaction kinetics, Atmos. Chem. Phys., 9, 8651–8660, 2009.

Lait, L. R.: An alternative form for potential vorticity, J. Atmos. Sci., 51, 1754–1759, 1994.

Lary, D. J.: Gas phase atmospheric bromine photochemistry, J. Geophys. Res., 101, 1505–1516, 1996.

Lary, D. J., Chipperfield, M. P., Toumi, R., and Lenton, T.: Heterogeneous atmospheric bromine chemistry, J. Geophys. Res., 101, 1489–1504, 1996.

Lehmann, R.: Determination of dominant pathways in chemical reaction systems: An algorithm and its Application to Stratospheric Chemistry, J. Atmos. Chem., 41, 297–314, 2002.

Lowe, D. and MacKenzie, A. R.: Polar stratospheric cloud microphysics and chemistry, J. Atmos. Solar-Terr. Phys., 70, 13–40, 2008.

Luo, B., Carslaw, K. S., Peter, T., and Clegg, S. L.: Vapour pressures of H_2SO_4/HNO_3/HCl/HBr/H_2O solutions to low stratospheric temperatures, Geophys. Res. Lett., 22, 247–250, 1995.

McElroy, M. B., Salawitch, R. J., Wofsy, S. C., and Logan, J. E.: Reductions of Antarctic ozone due to synergistic interactions of chlorine and bromine, Nature, 321, 759–762, 1986.

Molina, L. T. and Molina, M. J.: Production of Cl_2O_2 from the self-reaction of the ClO radical, J. Phys. Chem., 91, 433–436, 1987.

© Author(s) 2017. CC-BY 3.0 License.

Montzka, S. A.: Source gases that affect stratospheric ozone, in: Stratospheric Ozone Depletion and Climate Change, edited by Müller, R., chap. 2, pp. 33–77, RSC Publishing, 2012.

Müller, R., ed.: Stratospheric Ozone Depletion and Climate Change, RSC Publishing, Cambridge, 2011.

Nakajima, H., Wohltmann, I., Wegner, T., Takeda, M., Pitts, M. C., Poole, L. R., Lehmann, R., Santee, M. L., and Rex, M.: Polar Stratospheric Cloud evolution and chlorine activation measured by CALIPSO and MLS, and modelled by ATLAS, Atmos. Chem. Phys., 16, 3311–3325, 2016.

Peter, T. and Grooß, J.-U.: Polar Stratospheric Clouds and Sulfate Aerosol Particles: Microphysics, Denitrification and Heterogeneous Chemistry, in: Stratospheric Ozone Depletion and Climate Change, edited by Müller, R., chap. 4, pp. 108–144, RSC Publishing, 2012.

Pitts, M. C., Poole, L. R., Dörnbrack, A., and Thomason, L. W.: The 2009–2010 Arctic polar stratospheric cloud season: a CALIPSO perspective, Atmos. Chem. Phys., 11, 2161–2177, 2011.

Sander, S. P., Abbatt, J., Barker, J. R., Burkholder, J. B., Friedl, R. R., Golden, D. M., Huie, R. E., Kolb, C. E., Kurylo, M. J., Moortgat, G. K., Orkin, V. L., and Wine, P. H.: Chemical kinetics and photochemical data for use in atmospheric studies, Evaluation Number 17, JPL Publication 10-06, Jet Propulsion Laboratory, California Institute of Technology, Pasadena, http://jpldataeval.jpl.nasa.gov, 2011.

Solomon, S.: Stratospheric ozone depletion: A review of concepts and history, Rev. Geophys., 37, 275–316, 1999.

Solomon, S., Garcia, R. R., Rowland, F. S., and Wuebbles, D. J.: On the depletion of Antarctic ozone, Nature, 321, 755–758, 1986.

von Hobe, M. and Stroh, F.: Stratospheric halogen chemistry, in: Stratospheric Ozone Depletion and Climate Change, edited by Müller, R., chap. 2, pp. 78–107, RSC Publishing, 2012.

von Hobe, M., Bekki, S., Borrmann, S., Cairo, F., D'Amato, F., Di Donfrancesco, G., Dörnbrack, A., Ebersoldt, A., Ebert, M., Emde, C., Engel, I., Ern, M., Frey, W., Griessbach, S., Grooß, J.-U., Gulde, T., Günther, G., Hösen, E., Hoffmann, L., Homonnai, V., Hoyle, C. R., Isaksen, I. S. A., Jackson, D. R., Jánosi, I. M., Kandler, K., Kalicinsky, C., Keil, A., Khaykin, S. M., Khosrawi, F., Kivi, R., Kuttippurath, J., Laube, J. C., Lefèvre, F., Lehmann, R., Ludmann, S., Luo, B. P., Marchand, M., Meyer, J., Mitev, V., Molleker, S., Müller, R., Oelhaf, H., Olschewski, F., Orsolini, Y., Peter, T., Pfeilsticker, K., Piesch, C., Pitts, M. C., Poole, L. R., Pope, F. D., Ravegnani, F., Rex, M., Riese, M., Röckmann, T., Rognerud, B., Roiger, A., Rolf, C., Santee, M. L., Scheibe, M., Schiller, C., Schlager, H., Siciliani de Cumis, M., Sitnikov, N., Søvde, O. A., Spang, R., Spelten, N., Stordal, F., Sumińska-Ebersoldt, O., Viciani, S., Volk, C. M., vom Scheidt, M., Ulanovski, A., von der Gathen, P., Walker, K., Wegner, T., Weigel, R., Weinbuch, S., Wetzel, G., Wienhold, F. G., Wintel, J., Wohltmann, I., Woiwode, W., Young, I. A. K., Yushkov, V., Zobrist, B., and Stroh, F.: Reconciliation of essential process parameters for an enhanced predictability of Arctic stratospheric ozone loss and its climate interactions, Atmos. Chem. Phys., 13, 9233–9268, 2013.

Waters, J. W., Froidevaux, L., Harwood, R. S., Jarnot, R. F., Pickett, H. M., Read, W. G., Siegel, P. H., Coeld, R. E., Filipiak, M. J., Flower, D. A., Holden, J. R., Lau, G. K., Livesey, N. J., Manney, G. L., Pumphrey, H. C., Santee, M. L., Wu, D. L., Cuddy, D. T., Lay, R. R., Loo, M. S., Perun, V. S., Schwartz, M. J., Stek, P. C., Thurstans, R. P., Chandra, K. M., Chavez, M. C., Chen, G.-S., Boyles, M. A., Chudasama, B. V., Dodge, R., Fuller, R. A., Girard, M. A., Jiang, J. H., Jiang, Y., Knosp, B. W., LaBelle, R. C., Lam, J. C., Lee, K. A., Miller, D., Oswald, J. E., Patel, N. C., Pukala, D. M., Quintero, O., Scaff, D. M., Snyder, W. V., Tope, M. C., Wagner, P. A., and Walch, M. J.: The Earth Observing System Microwave Limb Sounder (EOS MLS) on the Aura satellite, IEEE Transactions on Geoscience and Remote Sensing, 44, 1075–1092, 2006.

Wayne, R. P., Poulet, G., Biggs, P., Burrows, J. P., Cox, R. A., Crutzen, P. J., Hayman, G. D., Jenkin, M. E., Bras, G. L., Moortgat, G. K., Platt, U., and Schindler, R. N.: Halogen oxides: Radicals, sources and reservoirs in the laboratory and in the atmosphere, Atmos. Environ., pp. 2677–2881, 1995.

© Author(s) 2017. CC-BY 3.0 License.

Wegner, T., Kinnison, D., Garcia, R., Madronich, S., Solomon, S., and von Hobe, M.: On the depletion of HCl in the Antarctic vortex, Geophys. Res. Abstracts, 15, 2013.

WMO: World Meteorological Organization (WMO) / United Nations Environment Programme (UNEP), Scientific assessment of ozone depletion: 2010, Global Ozone Research and Monitoring Project – Report No. 52, 2011.

Wohltmann, I. and Rex, M.: The Lagrangian chemistry and transport model ATLAS: validation of advective transport and mixing, Geosci. Model Dev., 2, 153–173, 2009.

Wohltmann, I., Lehmann, R., and Rex, M.: The Lagrangian chemistry and transport model ATLAS: simulation and validation of stratospheric chemistry and ozone loss in the winter 1999/2000, Geosci. Model Dev., 3, 585–601, 2010.

Wohltmann, I., Wegner, T., Müller, R., Lehmann, R., Rex, M., Manney, G. L., Santee, M. L., Bernath, P., Sumińska-Ebersoldt, O., Stroh, F., von Hobe, M., Volk, C. M., Hösen, E., Ravegnani, F., Ulanovsky, A., and Yushkov, V.: Uncertainties in modelling heterogeneous chemistry and Arctic ozone depletion in the winter 2009/2010, Atmos. Chem. Phys., 13, 3909–3929, 2013.

Wohltmann, I., Lehmann, R., and Rex, M.: Update of the SWIFT model for polar stratospheric ozone loss, Geophys. Model Dev., in preparation.